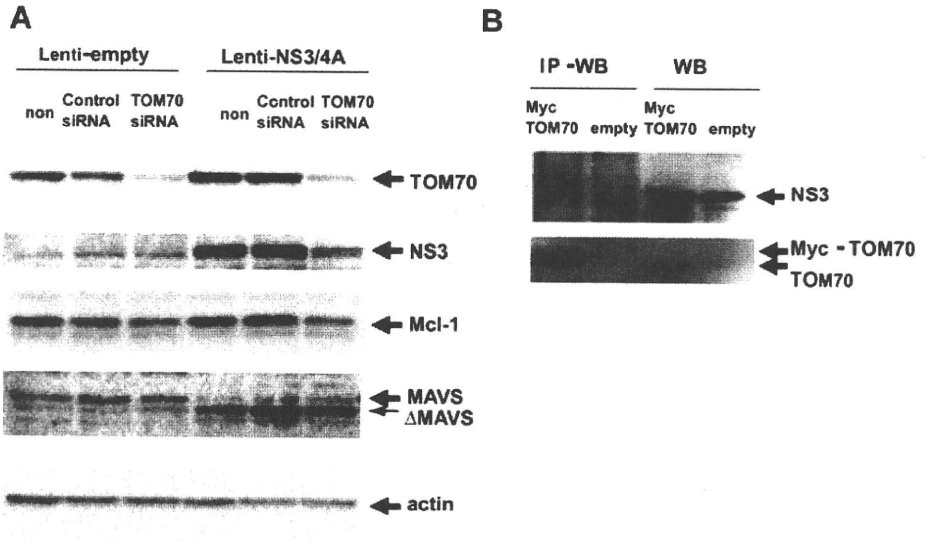

Fig. 3. Interaction between TOM70 and NS3 protein. **A**: The effect of TOM70 siRNA in cells transfected with empty or NS3/4A-containing lentivirus vectors was examined by WB with mAb 2-243a for TOM70; anti-NS3 rabbit polyclonal antibody; anti-Mcl-1 rabbit polyclonal antibody; anti-MAVS rabbit polyclonal antibody; and anti-actin antibody. **B**: The interaction between TOM70 and NS3 was assessed using IP-WB. NS3-expressing HepG2 cells were transfected with pcDNA6-TOM70 (mycTOM70) or pcDNA6 alone (empty) and immunoprecipitated with the anti-myc antibody (9E10). NS3 was detected using polyclonal rabbit anti-NS3 antibody (upper image), and TOM70 was detected using mAb 2-243a (lower image).

(Fig. 1A). p70 was induced to a greater extent by HCV expression after 8 days (RzM6-8d) or more than 44 days (RzM6-LC) than before HCV expression (RzM6-0d). The p70 expression level did not differ among the human hepatic cell lines (WRL68, HepG2, and HuH-7) (Fig. 1A, right panel). p70 was characterized (Fig. 1B–E): The sequence of peptides determined using MALDI-TOF-MS (Fig. 1B) and the MS/MS spectra of the p70 peptide sequence NVDLSTFYQNR (Fig. 1C) are provided. TOM70-pcDNA6 expression in HuH-7 cells was detected by WB with mAb 2-243a (Fig. 1D). Cell lysates were immunoprecipitated with anti-rat TOM70 antibody and detected by WB using mAb 2-243a (Fig. 1E). These results indicate that mAb 2-243a recognizes TOM70. Next, the effect of HCV infection on TOM70 expression was examined (Fig. 1F), and infection with the HCV JFH-1 strain [Wakita et al., 2005] induced TOM70 expression in HuH-7 cells (Fig. 1F). TOM70 localization was characterized using an indirect fluorescence assay (IFA) with 2-243a; anti-PDI, an ER marker; or MitoRed, which is a selective mitochondrial marker (Fig. 1G). TOM70 was associated with the mitochondria in all cells and was a part (~40%) of the ER, indicating that the TOM70 expressions in the mitochondria were higher than those in the ER.

TOM70 Inhibits TNF-α-Mediated Apoptotic Cell Death

The results of previous studies indicate the significant role of mitochondria in the apoptotic response [Hatano, 2007]. TOM70 interacts with Mcl-1 and facilitates mitochondrial targeting by the latter [Chou et al., 2006]. Mcl-1 silencing enhances TNF-related apoptosis-inducing ligand (TRAIL)-mediated cell death [Wirth et al., 2005; Han et al., 2006]. Therefore, the role of TOM70 in the apoptotic response was examined in this study. HepG2 cells were transfected with TOM70-pcDNA6 (Fig. 1D) or empty pcDNA6 (control), and their sensitivity to anti-Fas antibody (Fig. 2A) and TNF-α-mediated apoptotic cell death (Fig. 2B) was examined. When treated with 8 ng/ml of TNF-α, the TOM70-pcDNA6-transfected cells were significantly more viable than those transfected with empty pcDNA6 (Fig. 2B). In contrast, no significant differences were found between the viability of TOM70-pcDNA6 transfected cells and control cells treated with anti-Fas antibody (Fig. 2A). Thus, TNF-α-induced apoptosis was inhibited by TOM70 overexpression.

Interaction of TOM70 With HCV-NS3 and Other Host Factors

To determine the mechanism by which HCV induces TOM70, the TOM70 level in HCV NS3/4A-expressing HepG2 cells was determined (Fig. 3A). The TOM70 level was higher in the NS3/4A-expressing cells than in the control cells. Interestingly, the level of NS3/4A protein as well as Mcl-1 was reduced when TOM70 was silenced. The MAVS protein is cleaved by NS3/4A, as reported previously [Li et al., 2005], and the level of this protein was not influenced by the silencing of TOM70. IP-WB was performed to examine the possible interaction between TOM70 and NS3/4A (Fig. 3B). The pcDNA6-TOM70-myc plasmid was transfected into lenti-NS3/4A vector-transduced HepG2 cells; IP was performed using the anti-myc antibody, and the reaction was detected using the anti-NS3 antibody. The NS3 protein was

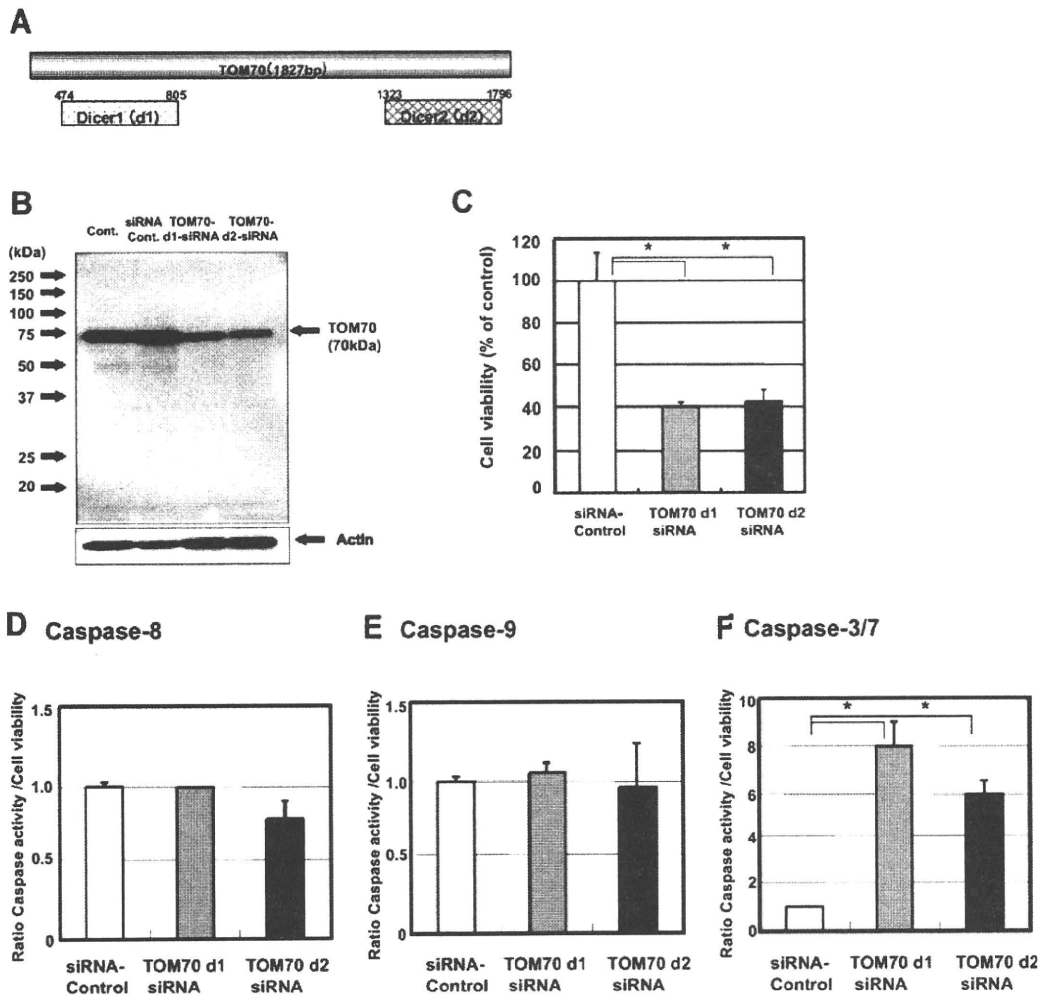

Fig. 4. Silencing of TOM70 induced apoptotic cell death and caspase-3/7 activity. **A**: The positions of TOM70-d1-siRNA and TOM70-d2-siRNA are indicated in the figure. **B**: siRNA-mediated silencing of TOM70 was detected by WB (Cont: no siRNA, siRNA Cont: siRNA control (Luci2-siRNA), TOM70-d1-siRNA, TOM70-d2-siRNA). **C**: TOM70 knockdown-induced cell death was calculated by measuring viability (%) with the WST-8 cell counting kit. The cell viability after 48 hr was scored in HepG2 cells transfected with the siRNA control Luci2-siRNA (□), TOM70-d1-siRNA (■), and TOM70-d2-siRNA (■). The activities of caspase-8 (**D**), caspase-9 (**E**), and caspase-3/7 (**F**) were measured using commercially available assays and a luminometer. The caspase activity was scored after 48 hr in TOM70-knockdown HepG2 cells transfected with control siRNA (□), TOM70-d1-siRNA (■), and TOM70-d2-siRNA (■). C–F: The data represent the average of the values obtained from triplicate experiments, and the vertical bars indicate the SD. $^*P < 0.05$ (two-tailed Student's t-test).

specifically precipitated by myc-tagged TOM70. The NS4A protein was not detected in this assay (data not shown). Therefore, the NS3 protein directly interacts with TOM70.

TOM70 Knockdown by RNAi Induces Apoptosis

The effect of TOM70 on the apoptotic response was examined because TOM70 silencing decreased the level of Mcl-1. First, two siRNAs for TOM70 (TOM70-d1-siRNA and TOM70-d2-siRNA) were designed in order to prevent the off-target effect (Fig. 4A). siRNA for luciferase (Luci-d2-siRNA) was used as a control (Fig. 4B). HepG2 cells were transfected with TOM70-d1-siRNA or TOM70-d2-siRNA, and the downregulation of TOM70 expression was confirmed by WB (Fig. 4B). Furthermore, decreased cell viability was observed (Fig. 4C) after 48 hr. Treatment with TOM70-d1-siRNA or TOM70-d2-siRNA significantly decreased the cell viability of HuH-7 cells too (data not shown). These results indicate that TOM70 silencing with siRNA may induce apoptosis.

The activities of caspase-3/7, caspase-8, and caspase-9 in HepG2 cells were examined after TOM70 silencing (Fig. 4D–F). The activities of caspase-8 and caspase-9 in cells transfected with TOM70 siRNA were not significantly different from those in the cells treated with control siRNA (Fig. 4D,E). In contrast, the caspase-3/7 activity in the TOM70-siRNA transfected cells was significantly greater than that in the cells treated with

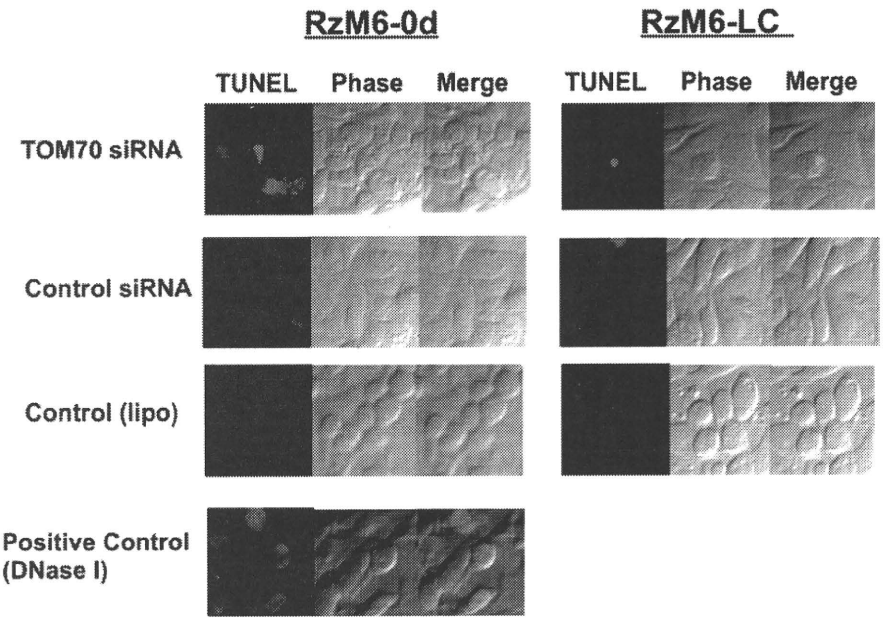

Fig. 5. TUNEL assay in RzM6-0d and RzM6-LC cells transfected with TOM70 siRNA, control siRNA, and control (Lipofectamine). The positive control is RzM6-0d cells treated with DNase I. The magnification is 400×.

control siRNA (Fig. 4F). These results indicate that the siRNA-mediated silencing of TOM70 expression induces apoptosis through caspase-3/7.

TOM70 Silencing-Induced Apoptosis Is Impaired by HCV

Next, the effect of TOM70 silencing-induced apoptosis was examined in RzM6-0d and RzM6-LC cells in order to determine the effect of HCV expression (Fig. 5). The apoptotic response was examined using the TUNEL assay wherein DNA strand breaks are detected and the apoptotic response is thereby detected [Gavrieli et al., 1992]. The DNA strand breaks, which were stained red, were observed using confocal microscopy. Treatment with TOM70 siRNA produced significant DNA strand breaks in the RzM6-0d cells. However, the apoptotic signal was suppressed in the RzM6-LC cells. This indicates the possibility that HCV can impair the apoptotic response induced by TOM70 siRNA.

Silencing of TOM70 Decreases Cell Viability, Whereas HCV-NS3 Restores Cell Viability

The RzM6-0d and RzM6-LC cells were treated with TOM70 siRNA and control siRNA, and the cell viability was measured using the WST-8 assay [Isobe et al., 1999] (Fig. 6A). The viability of the RzM6-LC cells was significantly higher than that of the RzM6-0d cells after treatment with TOM70 siRNA, and this difference increased in a dose-dependent manner. This indicates that the expression of HCV genes may impair the TOM70 siRNA-induced apoptotic response. The responsible HCV protein was identified using the lentivirus vector (Fig. 6B), and TOM70 siRNA-induced cell death was found to be impaired in HCV-NS3/4A-expressing cells.

DISCUSSION

The results of the present study suggest that HCV interacts with TOM70 through the NS3 protein, which indicates the possibility that TOM70 regulates the intracellular localization of HCV NS3; a previous study has reported the mitochondrion to be one of the regions where HCV NS3 is located [Sillanpaa et al., 2008]. The results of a previous study indicate that TOM70 also interacts with the Mcl-1 protein [Chou et al., 2006]. TOM70 silencing decreased the levels of the NS3 and Mcl-1 proteins; therefore, interaction with TOM70 may increase the stability of NS3 and Mcl-1. Recently, it was reported that Mcl-1 is stabilized by the deubiquitinase USP9X and that it can promote tumor cell survival [Schwickart et al., 2010]. Furthermore, Mcl-1 interacts with the HCV core protein through Bcl-2 homology domain 3 (BH3) [Mohd-Ismail et al., 2009], and Mcl-1 overexpression suppresses core-induced apoptosis. Therefore, further studies are required to clarify the relationship between TOM70, Mcl-1, and other host factors in HCV infection. This information may provide novel insights into the mechanism underlying the induction of apoptotic resistance and tumorigenicity in hepatocytes during chronic HCV infection.

The results of this study indicate the regulatory role of TOM70 in apoptosis. TOM70 overexpression was found to suppress the TNF-α-mediated but not the Fas-mediated apoptotic response. TOM70 knockdown

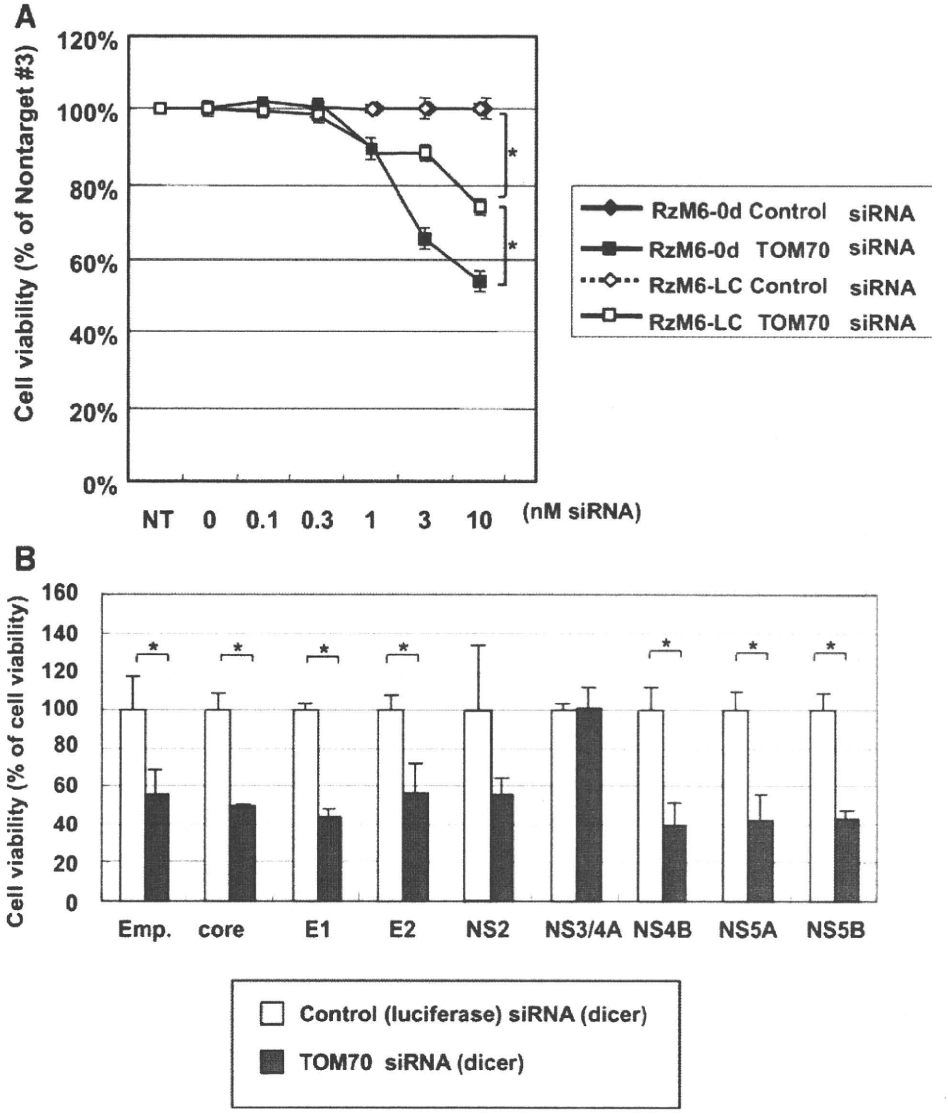

Fig. 6. **A**: Cell viability of RzM6-0d or RzM6-LC cells after treatment with TOM70 siRNA. The viability is given as the ratio (%) of test to control siRNA treatment. **B**: The viability of HepG2 cells transduced with lentivirus vectors expressing the HCV core, E1, E2, NS2, NS3/4A, NS4B, NS5A, and NS5B proteins after treatment with TOM70 siRNA was measured by the WST assay, and the viability is given as the ratio (%) of the test to the control siRNA treatment. The data represents the average of the values obtained from triplicate experiments, and the vertical bars indicate SD. $^{*}P < 0.05$ (two-tailed Student's t-test).

increased caspase-3/7 activity, but the activities of caspase-8 and caspase-9 were not significantly affected. This indicates the possibility that TOM70 regulates the TNF receptor-mediated apoptotic pathway. Several reports have indicated that TNF-α-mediated apoptosis is inhibited by HCV proteins. Saito et al. [2006] reported that the HCV core protein inhibited the TNF-α-mediated signaling pathway through the sustained expression of a cellular- FADD-like interleukin-1β-converting enzyme (FLICE) like inhibitory protein (c-FLIP; caspase-8 inhibitor). Majumder et al. [2002] reported that TNF-α-mediated hepatic apoptosis was impaired by the HCV-NS5A protein. The results of the present study revealed an alternative pathway by which HCV can acquire TNF-α-induced apoptotic resistance through TOM70 augmentation. Recently, it has been reported that TOM70 interacts with MAVS, TNFRSF1A-associated via death domain (TRADD), TNF receptor-associated factor 6 (TRAF6), stimulator of interferon genes (STING), and interferon regulatory factor (IRF)-3, and that augmentation of TOM70 activates retinoic acid-inducible gene (RIG)-I signaling [Liu et al., 2010]. The results of recent studies indicate that IRF-3 can activate Bax expression and apoptosis [Chattopadhyay et al., 2004]. Future studies on the modification of the regulatory pathway of TOM70 by HCV may provide further insights on the mechanism underlying persistent HCV infection.

ACKNOWLEDGMENTS

The authors thank Dr. H. Fukuda and Dr. S. Ohmi for their technical support with regard to MALDI-TOF-MS analysis, Dr. F. Yasui and Dr. T. Munakata for their critical comments, Dr. Satoh for his technical support, and Prof. S. Harada for his support.

REFERENCES

Chattopadhyay S, Marques JT, Yamashita M, Peters KL, Smith K, Desai A, Williams BR, Sen GC. 2004. Viral apoptosis is induced by IRF-3-mediated activation of Bax. EMBO J 29:1762–1773.

Chou CH, Lee RS, Yang-Yen HF. 2006. An internal EELD domain facilitates mitochondrial targeting of Mcl-1 via a Tom70-dependent pathway. Mol Biol Cell 17:3952–3963.

Deng L, Adachi T, Kitayama K, Bungyoku Y, Kitazawa S, Ishido S, Shoji I, Hotta H. 2008. Hepatitis C virus infection induces apoptosis through a Bax-triggered, mitochondrion-mediated, caspase 3-dependent pathway. J Virol 82:10375–10385.

Gavrieli Y, Sherman Y, Ben-Sasson SA. 1992. Identification of programmed cell death in situ via specific labeling of nuclear DNA fragmentation. J Cell Biol 119:493–501.

Han J, Goldstein LA, Gastman BR, Rabinowich H. 2006. Interrelated roles for Mcl-1 and BIM in regulation of TRAIL-mediated mitochondrial apoptosis. J Biol Chem 281:10153–10163.

Hatano E. 2007. Tumor necrosis factor signaling in hepatocyte apoptosis. J Gastroenterol Hepatol 22:S43–S44.

Hoogenraad NJ, Ward LA, Ryan MT. 2002. Import and assembly of proteins into mitochondria of mammalian cells. Biochim Biophys Acta 1592:97–105.

Isobe I, Michikawa M, Yanagisawa K. 1999. Enhancement of MTT, a tetrazolium salt, exocytosis by amyloid beta-protein and chloroquine in cultured rat astrocytes. Neurosci Lett 266:129–132.

Jensen ON, Wilm M, Shevchenko A, Mann M. 1999. Sample preparation methods for mass spectrometric peptide mapping directly from 2-DE gels. Methods Mol Biol 112:513–530.

Lei Y, Moore CB, Liesman RM, O'Connor BP, Bergstralh DT, Chen ZJ, Pickles RJ, Ting JP. 2009. MAVS-mediated apoptosis and its inhibition by viral proteins. PLoS One 4:e5466.

Li XD, Sun L, Seth RB, Pineda G, Chen ZJ. 2005. Hepatitis C virus protease NS3/4A cleaves mitochondrial antiviral signaling protein off the mitochondria to evade innate immunity. Proc Natl Acad Sci USA 102:17717–17722.

Liu XY, Wei B, Shi HX, Shan YF, Wang C. 2010. Tom70 mediates activation of interferon regulatory factor 3 on mitochondria. Cell Res 20:994–1011.

Majumder M, Ghosh AK, Steele R, Zhou XY, Phillips NJ, Ray R, Ray RB. 2002. Hepatitis C virus NS5A protein impairs TNF-mediated hepatic apoptosis, but not by an anti-FAS antibody, in transgenic mice. Virology 294:94–105.

Mihara K, Omura T. 1996. Cytoplasmic chaperones in precursor targeting to mitochondria: The role of MSF and hsp 70. Trends Cell Biol 6:104–108.

Mohd-Ismail NK, Deng L, Sukumaran SK, Yu VC, Hotta H, Tan YJ. 2009. The hepatitis C virus core protein contains a BH3 domain that regulates apoptosis through specific interaction with human Mcl-1. J Virol 83:9993–10006.

Neupert W. 1997. Protein import into mitochondria. Annu Rev Biochem 66:863–917.

Nishimura T, Kohara M, Izumi K, Kasama Y, Hirata Y, Huang Y, Shuda M, Mukaidani C, Takano T, Tokunaga Y, Nuriya H, Satoh M, Saito M, Kai C, Tsukiyama-Kohara K. 2009. Hepatitis C virus impairs p53 via persistent overexpression of 3beta-hydroxysterol Delta24-reductase. J Biol Chem 284:36442–36452.

Nomura-Takigawa Y, Nagano-Fujii M, Deng L, Kitazawa S, Ishido S, Sada K, Hotta H. 2006. Non-structural protein 4A of Hepatitis C virus accumulates on mitochondria and renders the cells prone to undergoing mitochondria-mediated apoptosis. J Gen Virol 87: 1935–1945.

Pfanner N, Geissler A. 2001. Versatility of the mitochondrial protein import machinery. Nat Rev Mol Cell Biol 2:339–349.

Pfanner N, Meijer M. 1997. The Tom and Tim machine. Curr Biol 7:R100–R103.

Saito K, Meyer K, Warner R, Basu A, Ray RB, Ray R. 2006. Hepatitis C virus core protein inhibits tumor necrosis factor alpha-mediated apoptosis by a protective effect involving cellular FLICE inhibitory protein. J Virol 80:4372–4379.

Saitou K, Mizumoto K, Nishimura T, Kai C, Tsukiyama-Kohara K. 2009. Hepatitis C virus-core protein facilitates the degradation of Ku70 and reduces DNA-PK activity in hepatocytes. Virus Res 144: 266–271.

Schatz G. 1996. The protein import system of mitochondria. J Biol Chem 271:31763–31766.

Schwickart M, Huang X, Lill JR, Liu J, Ferrando R, French DM, Maecker H, O'Rourke K, Bazan F, Eastham-Anderson J, Yue P, Dornan D, Huang DC, Dixit VM. 2010. Deubiquitinase USP9X stabilizes MCL1 and promotes tumour cell survival. Nature 463: 103–107.

Seeff LB. 2002. Natural history of chronic hepatitis C. Hepatology 36:S35–S46.

Sillanpaa M, Kaukinen P, Melen K, Julkunen I. 2008. Hepatitis C virus proteins interfere with the activation of chemokine gene promoters and downregulate chemokine gene expression. J Gen Virol 89:432–443.

Stojanovski D, Johnston AJ, Streimann I, Hoogenraad NJ, Ryan MT. 2003. Import of nuclear-encoded proteins into mitochondria. Exp Physiol 88:57–64.

Truscott KN, Pfanner N, Voos W. 2001. Transport of proteins into mitochondria. Rev Physiol Biochem Pharmacol 143:81–136.

Tsukiyama-Kohara K, Tone S, Maruyama I, Inoue K, Katsume A, Nuriya H, Ohmori H, Ohkawa J, Taira K, Hoshikawa Y, Shibasaki F, Reth M, Minatogawa Y, Kohara M. 2004. Activation of the CKI-CDK-Rb-E2F pathway in full genome hepatitis C virus-expressing cells. J Biol Chem 279:14531–14541.

Wakita T, Pietschmann T, Kato T, Date T, Miyamoto M, Zhao Z, Murthy K, Habermann A, Krausslich HG, Mizokami M, Bartenschlager R, Liang TJ. 2005. Production of infectious hepatitis C virus in tissue culture from a cloned viral genome. Nat Med 11: 791–796.

Wirth T, Kuhnel F, Fleischmann-Mundt B, Woller N, Djojosubroto M, Rudolph KL, Manns M, Zender L, Kubicka S. 2005. Telomerase-dependent virotherapy overcomes resistance of hepatocellular carcinomas against chemotherapy and tumor necrosis factor-related apoptosis-inducing ligand by elimination of Mcl-1. Cancer Res 65:7393–7402.

JLB

Article

Role of interleukin-18 in intrahepatic inflammatory cell recruitment in acute liver injury

Kiminori Kimura,[*,†,1] Satoshi Sekiguchi,[†] Seishu Hayashi,[*] Yukiko Hayashi,[‡] Tsunekazu Hishima,[‡] Masahito Nagaki,[§] and Michinori Kohara[†]*

Divisions of *Hepatology and [‡]Pathology, Tokyo Metropolitan Cancer and Infectious Diseases Center, Komagome Hospital, Tokyo, Japan; [†]Department of Microbiology and Cell Biology, Tokyo Metropolitan Institute of Medical Science, Tokyo, Japan; and [§]Department of Gastroenterology, Gifu University Graduate School of Medicine, Gifu, Japan

RECEIVED JULY 20, 2010; REVISED OCTOBER 12, 2010; ACCEPTED NOVEMBER 9, 2010. DOI: 10.1189/jlb.0710412

ABSTRACT

Although the innate immune system has been demonstrated to play important roles as the first line of defense against various infections, little is known about the interactions between intrahepatic inflammatory cells and the cytokine network in the liver. Here, we examined the role of IL-18 in IHL recruitment in acute liver injury. C57BL/6 mice were injected with an αCD40 mAb, and their serum IL-18 levels were observed to increase, with subsequent recruitment of IHLs into the liver. NKT cells were involved in this liver injury, as the serum ALT levels were reduced in NKT KO mice through the suppression of macrophage and monocyte migration and cytokine production. In contrast, depletion of neutrophils exacerbated the liver injury associated with high levels of TNF-α and IL-18 and increased numbers of macrophages and monocytes. Treatment with a neutralizing antibody against IL-18 reduced the serum ALT levels and inflammatory cell accumulation in the liver. Finally, additional administration of rIL-18 with αCD40 injection caused severe liver injury with increased IFN-γ production by NK cells. In conclusion, these findings demonstrate that IL-18 modulates liver inflammation by the recruitment of inflammatory cells, including NKT cells, macrophages, monocytes, and neutrophils. *J. Leukoc. Biol.* 89: 433–442; 2011.

Introduction

Macrophages of the innate immune system are the first line of defense against many pathogens and play a crucial role in the elimination of bacterial infections [1]. The resident liver macrophages, Kupffer cells, are well known to be phagocytic macrophages and account for 80% of the total population of fixed tissue macrophages in the body [2]. These cells are derived from blood monocytes and found mainly in the hepatic sinusoid [3]. They are continuously exposed to various pathogenic components, such as the gram-negative bacteria cell wall constituent LPS, and have the ability to protect their host immediately from the associated bacteria. Activated macrophages can also secrete inflammatory cytokines, such as TNF-α, IL-12, IL-18 [4, 5], and chemokines [6], in response to certain stimuli. These mediators produced by macrophages and the capacity for phagocytosis are essential for protection against microorganisms [7].

In contrast, NKT cells express an invariant TCR chain (V14-J281 in mice) and recognize glycolipid antigens, such as α-galactosylceramide, in association with the MHC class I-like molecule CD1d [8]. APCs, including DCs and macrophages, present antigens to NKT cells, a process that is dependent on CD40 ligation and results in the rapid release of large amounts of Th1 and Th2 cytokines and chemokines. Activated NKT cells can also provide maturation signals for other inflammatory cells, especially DCs, NK cells, and macrophages, thereby involving innate and acquired immunity [9, 10].

IL-18 is a member of the IL-1 family that is produced as a biologically inactive precursor and secreted after activation by cleavage with caspase-1 or other caspases [11]. Originally, IL-18 was identified as an IFN-γ-inducing factor that can act on Th1 cells, nonpolarized T cells, NK cells, B cells, and DCs to produce IFN-γ in the presence of IL-12 [12]. Besides its potent induction of IFN-γ, IL-18 activates NK and T cells, which play central roles in viral clearance [13].

We have already demonstrated that αCD40 mAb injection induces biphasic liver injury by way of inflammatory cytokine and chemokine production [14]. Furthermore, this liver injury requires NK cells and macrophages in the early-phase events, and B cells also contribute to the late-phase liver inflammation [15]. During analyses of this liver injury model, we found that

Abbreviations: αCD40=anti-CD40, ALT=alanine aminotransferase, IHL=intrahepatic leukocyte, KO=knockout (deficient), NLR=NOD-like receptor

The online version of this paper, found at www.jleukbio.org, includes supplemental information.

1. Correspondence: Division of Hepatology, Tokyo Metropolitan Cancer and Infectious Diseases Center, Komagome Hospital, 18-22-3 Honkomagome, Bunkyo-ku, Tokyo 113-8677, Japan. E-mail: kkimura@cick.jp

serum IL-18 was increased dramatically at the late phase. In the present study, we investigated the involvement of IL-18 in the liver injury and focused on the interactions among IL-18 and NKT cells, neutrophils, macrophages, and monocytes, which play important roles in various diseases. The results obtained provide new insights into the inflammatory network among macrophages, neutrophils, and NKT cells during liver injury.

MATERIALS AND METHODS

Mice

Vα14 NKT KO mice were generated as described [7], and C57BL/6 mice were purchased from Japan SLC (Shizuoka, Japan). All animals were housed in pathogen-free rooms under strict barrier conditions and received humane care according to the guidelines of the Animal Care Committees of Gifu University School of Medicine (Gifu, Japan) and Tokyo Metropolitan Institute of Medical Science (Tokyo, Japan).

Antibodies

Mice were injected i.v. with 100 μg αCD40 [16] or 100 μg purified rat IgG2a as a control (BD PharMingen, San Diego, CA, USA). In addition, some mice were injected i.p. (200 μg/mouse) at Days −1, +1, and +3 with a rat mAb against mouse Gr-1 (clone RB6-8C5) and control rat IgG2b (both from eBioscience, San Diego, CA, USA). At Days −1, +1, and +3, other mice were injected i.p. with a rat anti-mouse IL-18 mAb (50 μg/mouse) and rat IgG (both from MBL, Nagoya, Japan).

Cell isolation

To isolate IHLs, single-cell suspensions were prepared from liver perfused with PBS via the inferior vena cava and digested in 10 mL RPMI 1640 (Life Technologies, Gaithersburg, MD, USA) containing 0.02% (wt/vol) collagenase IV (Sigma-Aldrich, St. Louis, MO, USA) and 0.002% (wt/vol) DNase I (Sigma-Aldrich) for 40 min at 37°C. Cells were overlaid on Lympholyte M (Cedarlane, Westbury, NY, USA) in PBS. Bone marrow cells were collected from the femurs and tibias of mice. To isolate PBMCs, peripheral blood (0.4 mL) was obtained by cardiac puncture under ether anesthesia. After density separation, cell counts and immunofluorescence analyses were performed.

Tissue RNA analyses

Frozen livers were mechanically pulverized under liquid nitrogen, and total RNAs were isolated for RPAs as described previously [15]. All reagents for the RPAs were purchased from BD PharMingen.

ELISA

The serum IL-18, TNF-α, and IFN-γ concentrations were assayed using specific ELISA kits (IL-18, MBL; TNF-α and IFN-γ, Genzyme Techne Corp., Minneapolis, MN, USA), according to each corresponding manufacturer's protocols.

Immunohistochemistry

The samples were embedded in OCT compound (Tissue Tek, Miles, Elkhart, IN, USA) and frozen in liquid nitrogen. Sections were cut at 4 μm thickness using a cryostat and fixed with cold acetone for 10 min. The fixed sections were treated with rat anti-mouse F4/80, Ly-6C, and Gr-1 mAb (10 μg/mL), followed by a streptavidin-biotin-HRP complex (Dako, Glostrup, Denmark). The positive reactions were visualized with 0.035% H_2O_2 and 0.03% 3,3′-diaminobenzidine (Wako, Tokyo, Japan) in 50 mM Tris-HCl (pH 7.6) for 2–3 min. After 4% formaldehyde fixation, the stained sections were counterstained with hematoxylin and subjected to microscopic observation.

Flow cytometry

The cells were surface-stained with fluorochrome-conjugated mAb for 20 min on ice. The following antibodies were used: anti-CD3, anti-NK1.1, anti-CD11b, and anti-CD11c (all from eBioscience). The F4/80 and Ly-6C mAb (BMA Biomedicals, Geneva, Switzerland) were also used. In addition, the cells were surface-stained with FITC-conjugated anti-CD3, FITC-conjugated anti-CD11b, and allophycocyanin-conjugated anti-NK1.1 mAb, together with anti-IFN-γ-PE and anti-TNF-α-PE mAb (all from BD PharMingen) for intracellular cytokine detection. Samples were acquired using a FACSCalibur flow cytometer, and data were analyzed using the CellQuest software (BD Immunocytometry Systems, San Jose, CA, USA) and FlowJo software (Tree Star, San Carlos, CA, USA).

BrdU incorporation

For in vivo BrdU labeling, mice received a 100-μL i.p. injection of a 10-mg/mL solution of BrdU in PBS at 2 h before sacrifice. Single-cell suspensions of IHLs were prepared at 24 h after αCD40 injection and surface-stained with PE-CD11b. Following the surface staining, the cells were fixed, stained for intracellular BrdU using a FITC-BrdU flow kit (BD PharMingen), and analyzed by flow cytometry.

Data analysis

All data are expressed as the mean + SD. Values of $P < 0.05$ were considered statistically significant.

RESULTS

A single injection of αCD40 increases serum IL-18

We found that the serum ALT activity began to elevate on Day 1 and was clearly increased on Day 5 after αCD40 injection. We confirmed further that inflammatory cytokine and chemokine mRNA expressions were increased at Days 1 and 5 in C57BL/6 mice (Supplemental Fig. 1A). We measured the serum IL-18 level and found that it began to increase at Day 3 and was remarkably increased until Day 5 after the injection. To determine the infiltration of inflammatory cells in the same livers, we counted the absolute number of IHLs and calculated the number of cells in each IHL subset. As shown in **Fig. 1B**, Gr-1^{++}/CD11b^{+} cells (mostly neutrophils) were increased until Day 1 and then decreased at Days 3 and 5. On the other hand, Gr-1^{+}/CD11b^{+} cells (mostly macrophages and monocytes) were increased and reached a peak at Day 3 and then decreased until Day 5. Furthermore, to evaluate the numbers of macrophages and their precursors in the liver, the cells were stained with the CD11b, F4/80, and Ly-6C mAb, which recognize antigens on macrophages and their precursors at different stages of differentiation [17]. The numbers of Ly-6C^{++}/CD11b^{+} cells (mostly monocytes) and F4/80^{+}/CD11b^{+} cells (tissue macrophages) began to increase by Day 1, reached a peak at Day 3, and then decreased until Day 5. In immunohistochemical analyses, Gr-1^{+} cells were increased at Day 1 in the liver parenchyma, whereas Ly-6C^{+} and F4/80^{+} cells were increased at Day 3 in the liver (Fig. 1C), consistent with the FACS data.

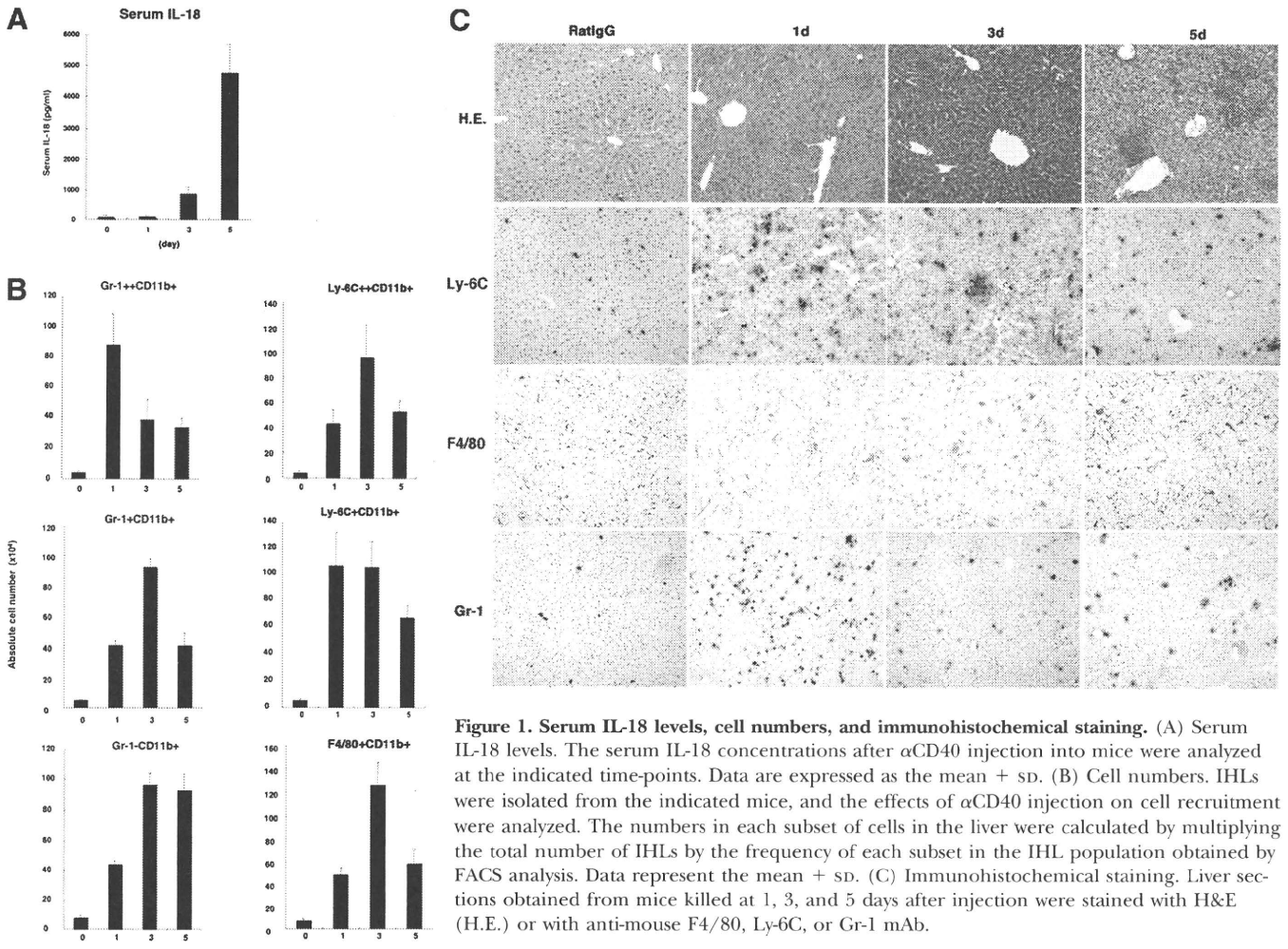

Figure 1. Serum IL-18 levels, cell numbers, and immunohistochemical staining. (A) Serum IL-18 levels. The serum IL-18 concentrations after αCD40 injection into mice were analyzed at the indicated time-points. Data are expressed as the mean + SD. (B) Cell numbers. IHLs were isolated from the indicated mice, and the effects of αCD40 injection on cell recruitment were analyzed. The numbers in each subset of cells in the liver were calculated by multiplying the total number of IHLs by the frequency of each subset in the IHL population obtained by FACS analysis. Data represent the mean + SD. (C) Immunohistochemical staining. Liver sections obtained from mice killed at 1, 3, and 5 days after injection were stained with H&E (H.E.) or with anti-mouse F4/80, Ly-6C, or Gr-1 mAb.

Proliferation and differentiation of macrophages after αCD40 injection

As reported previously [14], macrophages were key players in this liver injury. We confirmed that αCD11b mAb treatment suppressed inflammatory cytokine and chemokine expressions in the liver and the serum IL-18 levels (Supplemental Fig. 2A and B), indicating that macrophages are IL-18 producers, consistent with a previous report [11].

Next, to evaluate the function of macrophages after αCD40 injection, we analyzed the proliferation of macrophages by BrdU staining in the liver, bone marrow, and PBMCs. We injected 2 mg BrdU i.p. into mice at 2 h before sacrifice. Proliferation of $CD11b^+$ cells peaked in each tissue at Day 3 after injection and decreased by Day 5 (**Fig. 2A**), consistent with the numbers of the macrophage populations in the FACS analysis.

To determine whether differentiation from monocytes to tissue macrophages was induced in each tissue, we investigated the changes in the proportions of $Ly\text{-}6C^+$ and $F4/80^+$ cells among the $CD11b^+$ cells (Fig. 2B). $Ly\text{-}6C^-/F4/80^+/CD11b^+$ and $Ly\text{-}6C^+/F4/80^-/CD11b^+$ cells comprised the majority of cells in the liver after injection of the control antibody, and $Ly\text{-}6C^+/F4/80^+/CD11b^+$ cells increased at Day 1 and peaked at Day 3. These findings demonstrate that the proportion of $Ly\text{-}6C^-/F4/80^+/CD11b^+$ cells increased from Days 3 to 5, indicating that differentiation from monocytes to tissue macrophages had occurred by Day 3. In the bone marrow, $Ly\text{-}6C^+/F4/80^+/CD11b^+$ cells began to increase at Day 1 after αCD40 injection compared with the findings for the control antibody but had decreased by Day 5, indicating that αCD40 stimulation also induced the differentiation of macrophages. Similarly, $Ly\text{-}6C^+/F4/80^+/CD11b^+$ cells, among the PBMCs, began to increase by Day 1 after αCD40 injection and peaked at Day 3.

Role of NKT cells

To evaluate the role of NKT cells in this liver injury, NKT KO and C57BL/6 mice were injected with αCD40 and killed at Days 1 and 5. No significant difference between the serum ALT activities was observed after rat IgG injection, which is presented as Day 0, and NKT KO mice exhibited significantly lower serum ALT activities than WT mice at Days 1 and 5 ($P<0.05$; **Fig. 3A**). We also found that the absolute numbers of NK cells, T cells, macrophages, and neutrophils among the IHLs were reduced significantly in NKT KO mice (Fig. 3B). Consistent with the reduced number of IHLs in NKT KO mice, the IFN-γ, TNF-α, CCL2, and CCL5 mRNA expressions in the liver were suppressed at Days 1 and 5 after αCD40 injection (Fig. 3C and

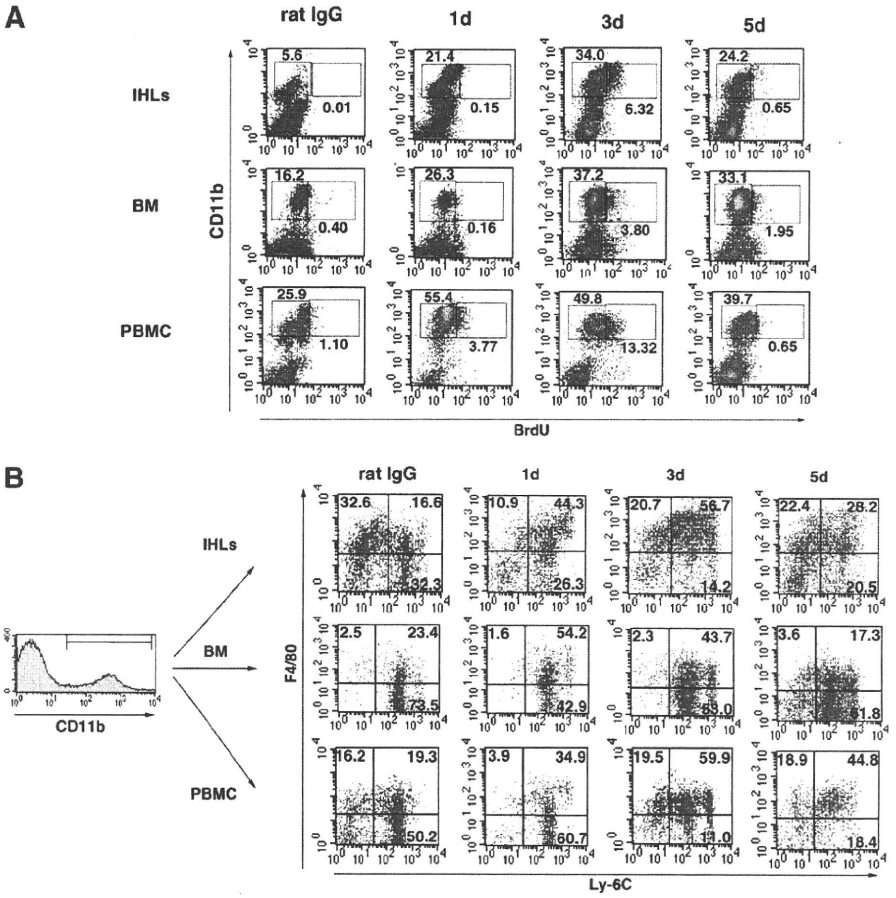

Figure 2. Macrophage differentiation and proliferation after αCD40 injection. (A) To analyze macrophage proliferation in IHLs, bone marrow (BM), and PBMCs after αCD40 injection, C57BL/6 mice were injected i.p. with 2 mg BrdU at 2 h before sacrifice. Cells were stained with anti-CD11b-allophycocyanin and anti-BrdU-FITC antibodies. (B) To analyze macrophage differentiation in IHLs, bone marrow, and PBMCs, cells were stained with anti-CD11b-allophycocyanin, anti-mouse F4/80-FITC, and anti-mouse Ly-6C-PE mAb.

D). We further found that the IFN-γ production by NK cells and TNF-α production by macrophages were suppressed in NKT KO mice (**Supplemental Fig. 3**). Furthermore, the serum IL-18 levels were reduced in NKT KO mice at Day 5 but not Day 1.

Finally, the numbers of Ly-6C^{++}/CD11b^{+}, Ly-6C^{+}/CD11b^{+}, and F4/80^{+}/CD11b^{+} cells in NKT KO mice were reduced significantly compared with WT mice at Day 5 after injection (Fig. 3E), demonstrating that NKT cells were involved in the macrophage and monocyte infiltration in the liver.

Depletion of neutrophils exacerbates the liver injury

To determine whether neutrophils play a role in this liver injury, we injected αCD40 into C57BL/6 mice with αGr-1 mAb or rat IgG2b at Days −1, +1, and +3. The mice were killed at Day 5. We confirmed that αGr-1 mAb treatment specifically depleted IHLs with an efficiency of >95% (Gr-1^{++}/CD11b^{+} cells), as evaluated by FACS analysis (Supplemental Fig. 4).

Administration of αGr-1 mAb significantly increased the serum ALT activity at Day 5 compared with the control antibody (P<0.05; **Fig. 4A**). Although the total number of IHLs decreased after αCD40 plus αGr-1 mAb treatment, the numbers of Gr-1^{+}/CD11b^{+} cells, including Ly-6C^{++}/CD11b^{+} and F4/80^{+}/CD11b^{+} cells, increased (Fig. 4B, C, and E). Immunohistochemical analyses revealed that Ly-6C^{+} and F4/80^{+} cells were increased in the liver at Day 5 after αCD40 mAb plus αGr-1 mAb treatment (Fig. 4F). Consistent with these observations, the serum TNF-α and IL-18 but not IFN-γ levels were elevated in the neutrophil-depleted state (Fig. 4D). In addition, TNF-α production by Ly-6C^{++}/CD11b^{+} and F4/80^{+}/CD11b^{+} cells was increased in αGr-1 mAb-treated mice (Fig. 4G), suggesting that neutrophils may play a suppressive role in macrophage recruitment and function in this liver inflammation.

Neutralization of IL-18 suppresses the liver injury

To assess whether IL-18 is responsible for the αCD40-induced liver injury, we injected C57BL/6 mice with αIL-18 mAb or rat IgG as a control at −1, +1, and 2 days after αCD40 injection and then killed the mice at Day 5. Administration of αIL-18 mAb significantly suppressed the serum ALT activity at Day 5 (P<0.05; **Fig. 5A**), demonstrating that IL-18 contributes to the liver injury. Consistent with this finding, αIL-18 mAb treatment decreased the IFN-γ and TNF-α mRNA expressions in the liver (Fig. 5B). We also found that αIL-18 mAb treatment inhibited the recruitment of macrophage subpopulations, neutrophils, NK cells, and T cells but not NKT cells into the liver (Fig. 5C). Immunohistochemical analyses revealed that Ly-6C^{+} and F4/80^{+} cells

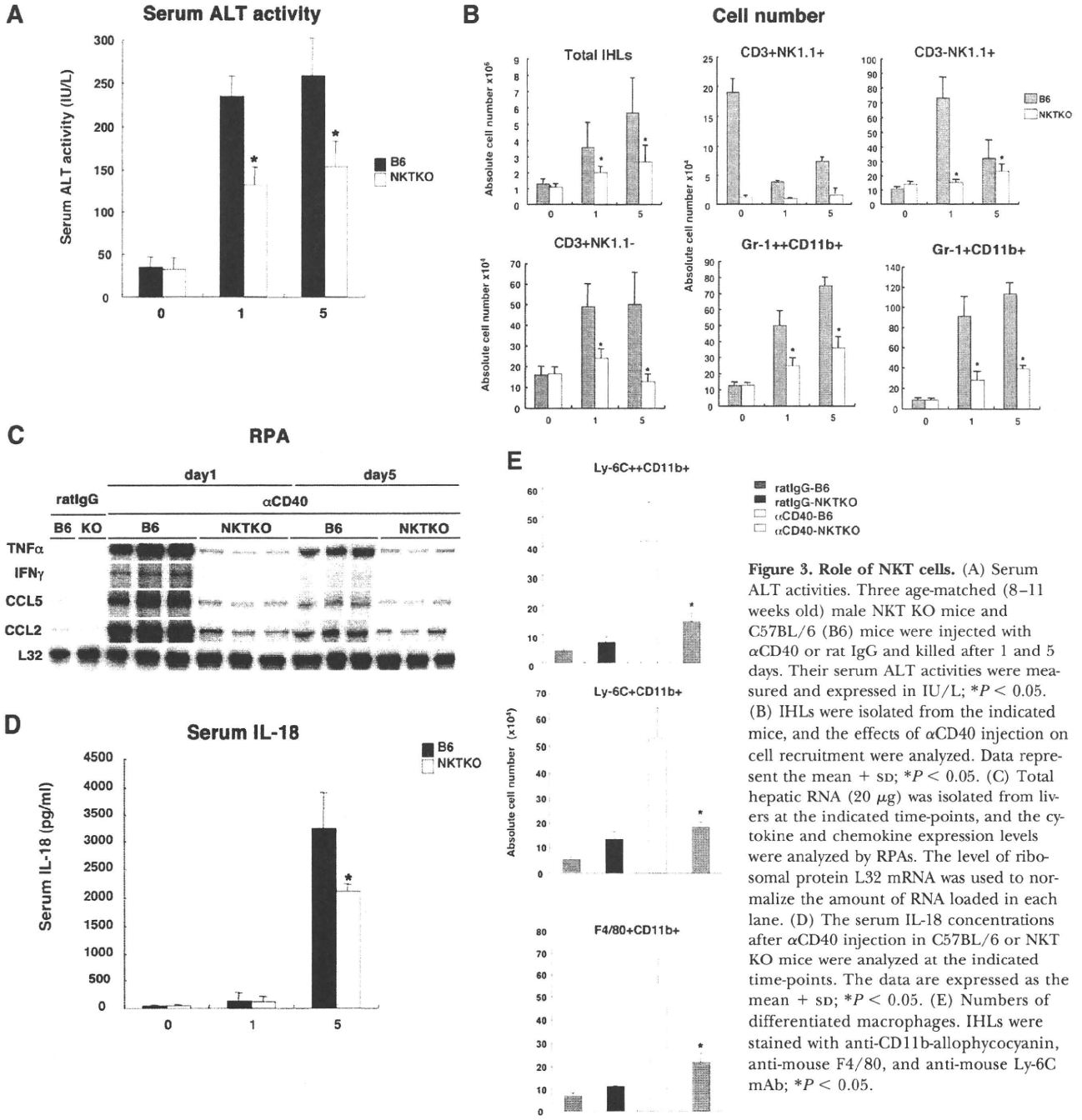

Figure 3. Role of NKT cells. (A) Serum ALT activities. Three age-matched (8–11 weeks old) male NKT KO mice and C57BL/6 (B6) mice were injected with αCD40 or rat IgG and killed after 1 and 5 days. Their serum ALT activities were measured and expressed in IU/L; $*P < 0.05$. (B) IHLs were isolated from the indicated mice, and the effects of αCD40 injection on cell recruitment were analyzed. Data represent the mean + SD; $*P < 0.05$. (C) Total hepatic RNA (20 μg) was isolated from livers at the indicated time-points, and the cytokine and chemokine expression levels were analyzed by RPAs. The level of ribosomal protein L32 mRNA was used to normalize the amount of RNA loaded in each lane. (D) The serum IL-18 concentrations after αCD40 injection in C57BL/6 or NKT KO mice were analyzed at the indicated time-points. The data are expressed as the mean + SD; $*P < 0.05$. (E) Numbers of differentiated macrophages. IHLs were stained with anti-CD11b-allophycocyanin, anti-mouse F4/80, and anti-mouse Ly-6C mAb; $*P < 0.05$.

were decreased in the liver at Day 5 after αCD40 mAb plus αIL-18 mAb treatment (Fig. 5D).

IL-18 causes severe liver injury with high levels of IFN-γ

To evaluate the effect of IL-18 on the late-phase liver injury, we i.p.-injected mice with 1 μg murine rIL-18 at 4 days after αCD40 injection and measured their serum ALT activity and inflammatory cytokine levels. The serum ALT activity was increased significantly by about four times after rIL-18 treatment compared with the control, although the number of IHLs, except for the macrophage population, was suppressed (**Fig. 6A–C**). In addition, serum IFN-γ was elevated significantly after injection of αCD40 with rIL-18, and NK cells strongly produced IFN-γ after rIL-18 treatment (Fig. 6D and E). In contrast, no difference was seen for TNF-α production by macrophages (Fig. 6E). Thus, IL-18 mainly activated NK cells and reduced the numbers of monocytes and neutrophils in the liver (Fig. 6A and B).

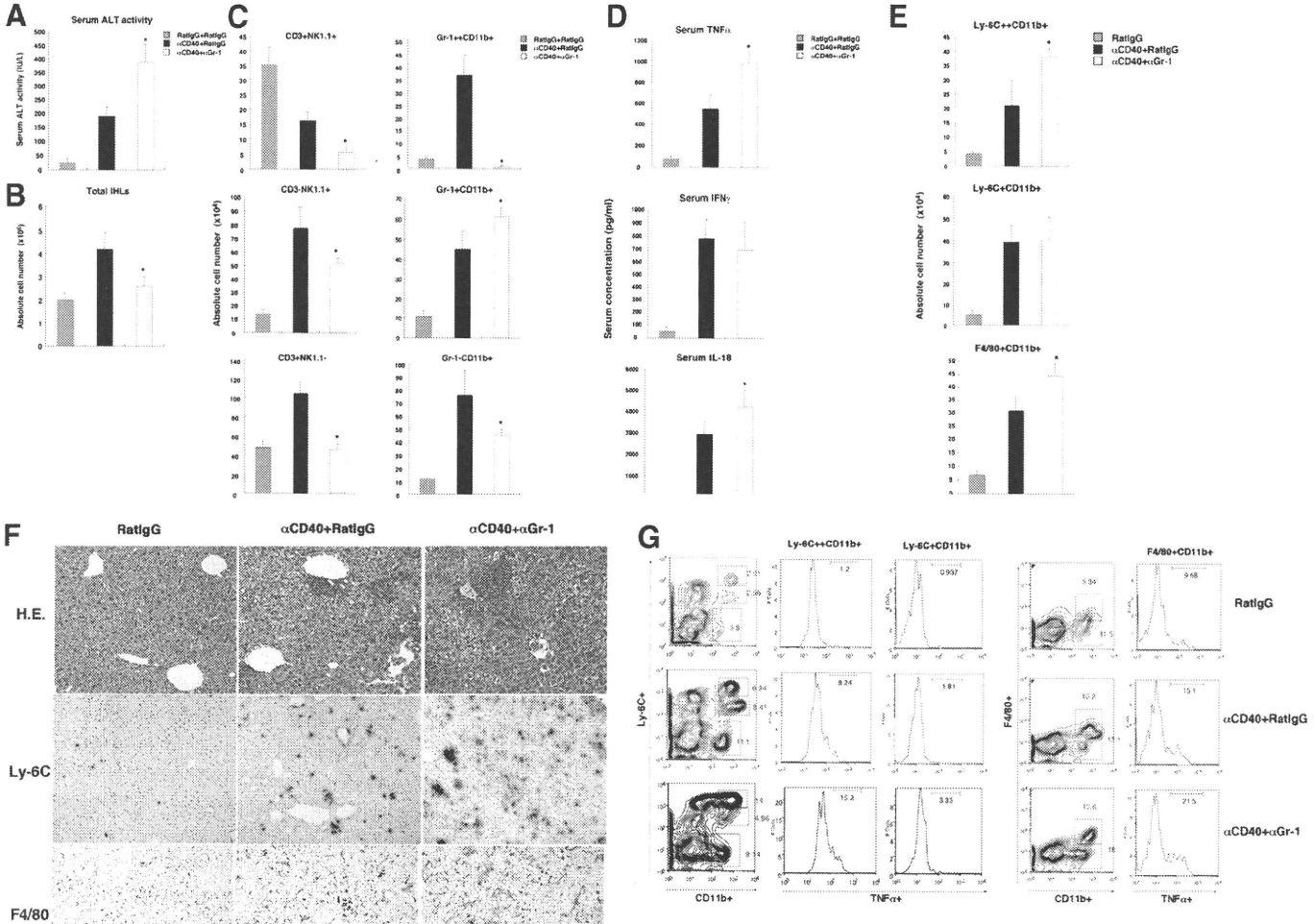

Figure 4. Role of neutrophils. (A) Serum ALT activities. C57BL/6 mice were injected with αCD40 or rat IgG in the absence or presence of αGr-1 mAb and killed after 5 days. Their serum ALT activities were measured and expressed in IU/L; $*P < 0.05$. (B and C) IHLs were isolated from the indicated mice, and the effects of αGr-1 mAb on cell recruitment were analyzed. Data represent the mean + SD; $*P < 0.05$. (D) Serum cytokine concentrations after αCD40 injection in C57BL/6 mice. Data are expressed as the mean + SD; $*P < 0.05$. (E) Numbers of differentiated macrophages. IHLs were stained with anti-CD11b-allophycocyanin, anti-mouse F4/80, and anti-mouse Ly-6C mAb; $*P < 0.05$. (F) Immunohistochemical staining. Liver sections obtained from mice killed at 5 days after injection were stained with H&E or with anti-mouse F4/80, Ly-6C, or Gr-1 mAb. (G) Intracellular cytokine expression levels in macrophages and monocytes. To determine which cell populations produced TNF-α after injection, we stained the cells with anti-mouse F4/80-FITC, Ly-6C-PE, anti-CD11b-allophycocyanin, and anti-TNF-α-PE mAb. The cells were analyzed using a FACSCalibur system.

DISCUSSION

The present study has clarified several important aspects of liver pathology in terms of inflammatory cell recruitment and activation in the liver and provides important findings regarding the interactions among IL-18, macrophages, neutrophils, and NKT cells. The innate immune system, which is considered to provide nonantigen-specific immune responses, can provide emergency signals from destroyed hepatocytes during liver inflammation, resulting in an inflammatory response. These inflammatory events contribute to liver injury and conversely, may also be involved in liver repair based on various experimental liver disease models [18–20]. Therefore, it is well established that an inflammatory response is essential for controlling the microenvironment in the liver, but the relationships among macrophages and other inflammatory cells with regard to liver injury are still obscure. Careful interpretation is required to evaluate the results of the present study, especially with regard to the interactions between IHLs and the liver injury in this model. The liver injury model that we used involves artificial stimulation of macrophages, monocytes, and B cells that express CD40, and these cells subsequently activate NK cells and NKT cells, thereby causing liver injury by way of IFN-γ, TNF-α, and IL-12 [14, 15]. In general, it has

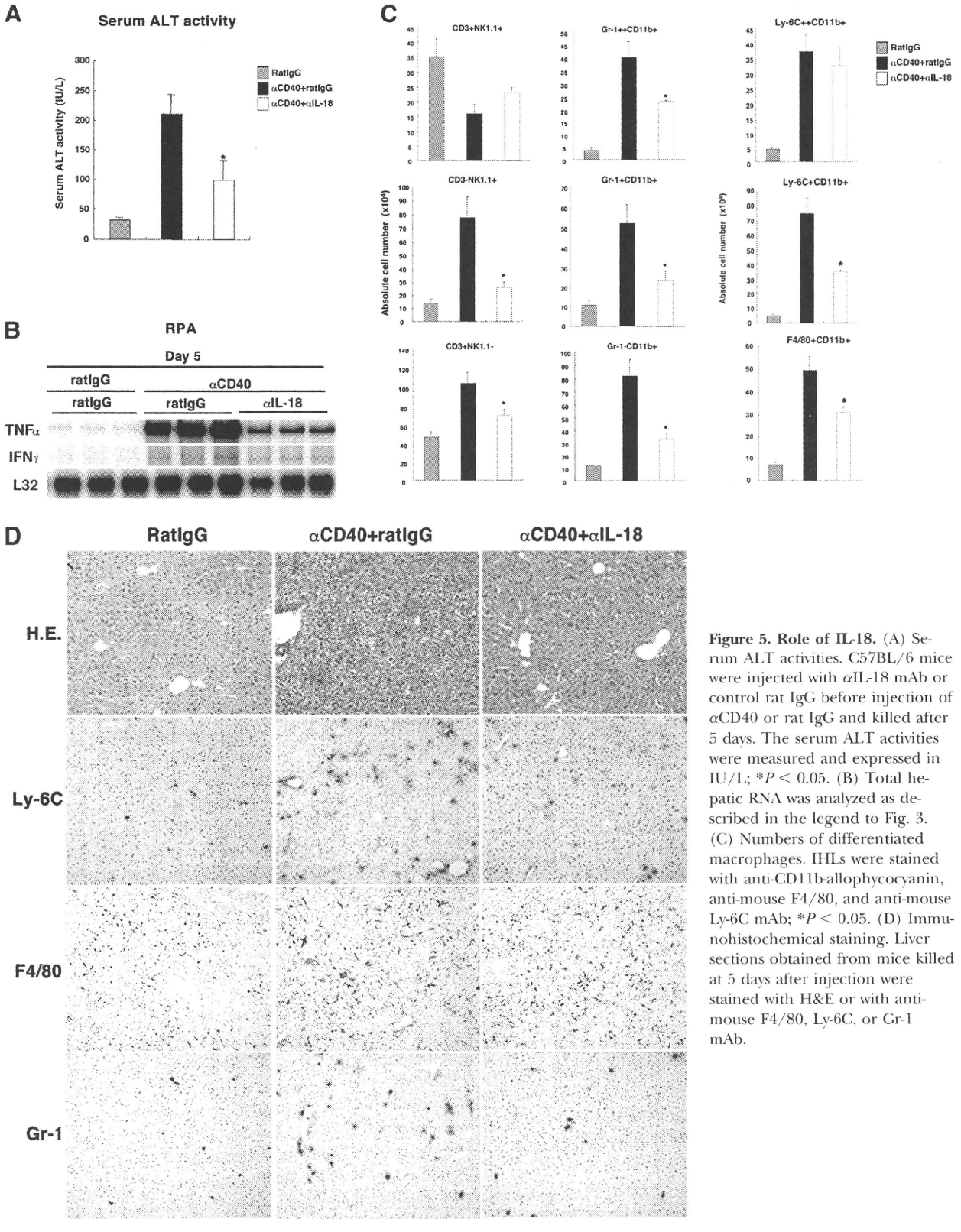

Figure 5. Role of IL-18. (A) Serum ALT activities. C57BL/6 mice were injected with αIL-18 mAb or control rat IgG before injection of αCD40 or rat IgG and killed after 5 days. The serum ALT activities were measured and expressed in IU/L; $*P < 0.05$. (B) Total hepatic RNA was analyzed as described in the legend to Fig. 3. (C) Numbers of differentiated macrophages. IHLs were stained with anti-CD11b-allophycocyanin, anti-mouse F4/80, and anti-mouse Ly-6C mAb; $*P < 0.05$. (D) Immunohistochemical staining. Liver sections obtained from mice killed at 5 days after injection were stained with H&E or with anti-mouse F4/80, Ly-6C, or Gr-1 mAb.

been well understood that the interactions between CD40 and CD40 ligand reciprocally deliver activating signals to APCs and cognate T cells. This process is critically important for the development of adaptive immunity [21–23]. However, we consider that this liver injury model is useful for analyzing how activated macrophages or B cells affect the activation of other IHLs and their recruitment in liver injury, as the agonistic CD40 antibody mainly activates macrophages and B cells.

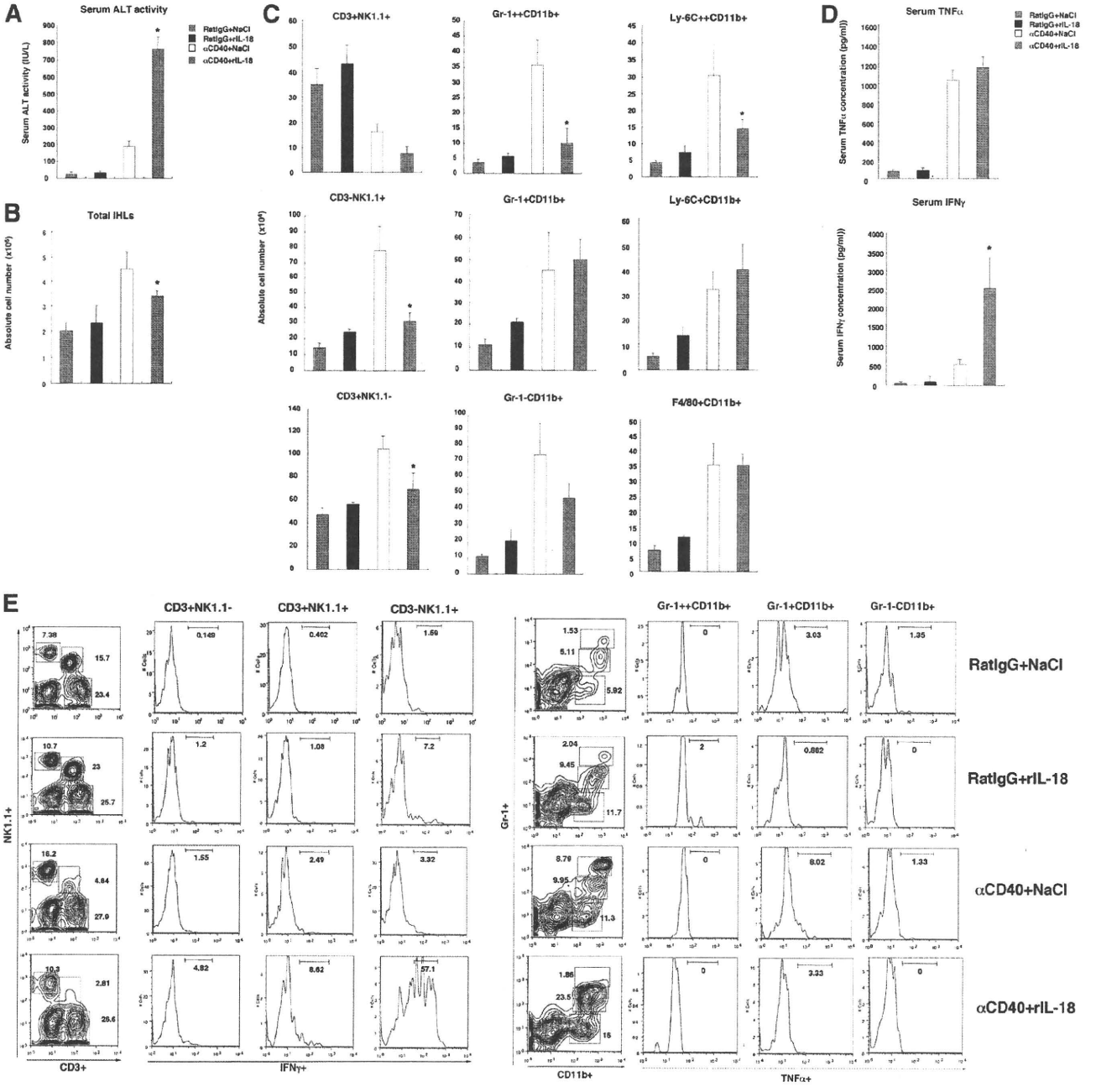

Figure 6. Additional IL-18 treatment exacerbates liver injury after αCD40 injection. (A) Serum ALT activities. C57BL/6 mice were injected with αCD40 or rat IgG in the absence or presence of rIL-18 and killed after 5 days. The serum ALT activities were measured and expressed in IU/L; $*P < 0.05$. (B and C) IHLs were isolated from the indicated mice, and the effects of IL-18 on cell recruitment were analyzed. Data represent the mean + SD; $*P < 0.05$. (D) Serum cytokine concentrations after αCD40 injection in C57BL/6 mice. Data are expressed as the mean + SD; $*P < 0.05$. (E) Intracellular cytokine expression levels in macrophages and monocytes. To determine which cell populations produced TNF-α after injection, we stained the cells with anti-mouse F4/80-FITC, Ly-6C-PE, anti-CD11b-allophycocyanin, and anti-TNF-α-PE mAb. The cells were analyzed using a FACSCalibur system.

First, we determined the characteristics of intrahepatic macrophages, which became activated on Days 1 and 5 after αCD40 injection, as they are key effector cells for the liver injury [14]. We analyzed the proliferation of the macrophages and detected a peak at Day 3. This finding was consistent with the observed numbers of macrophages. Notably, the highly proliferating macrophages were unable to produce TNF-α, and this is considered to be one of the reasons why αCD40-triggered inflammation exhibits a biphasic pattern in the liver. The present study demonstrated that monocyte subsets differing in Ly-6C expression represented different stages in

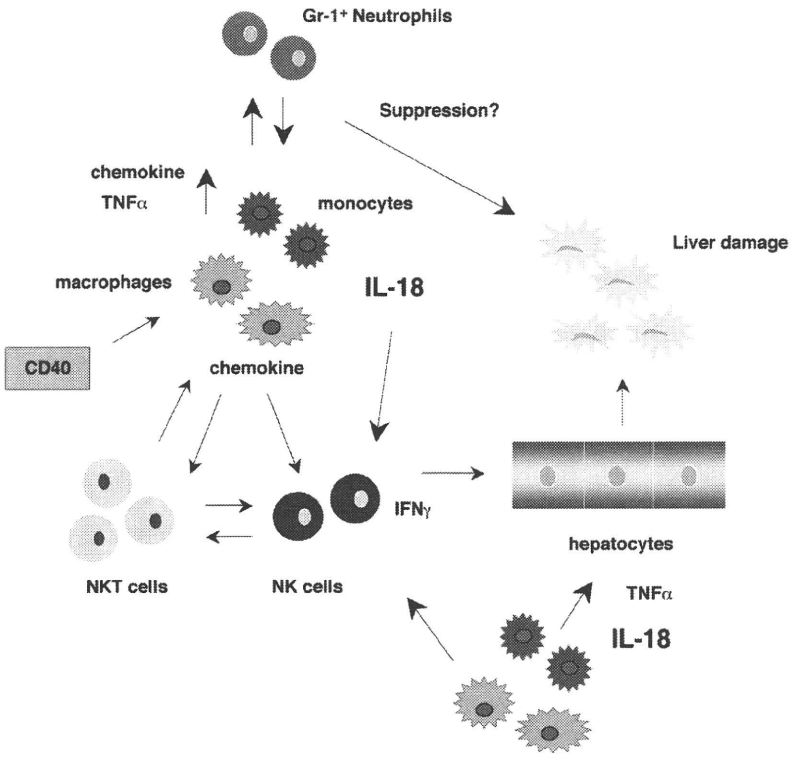

Figure 7. Scheme for how αCD40 triggers liver inflammation. 1) TNF-α and chemokines are produced by activated macrophages after αCD40 stimulation. 2) Neutrophils increase rapidly and control the activation of macrophages or monocytes. 3) At the same time, NKT cells are activated and produce inflammatory cytokines. 4) IL-18 stimulates the migration of macrophages and monocytes into the liver and activates NK cells. 5) Inflammatory cytokines stimulate IFN-γ production by NK cells, and the produced IFN-γ further stimulates macrophages and exacerbates the severe liver injury.

a continuous maturation pathway, and previous in vitro experiments indicated that this transition occurs within 24–48 h [24]. Based on these findings, we suggest that not only the increase in Ly-6C^{high} monocytes, which have suppressive functions [25], but also the high proliferation of macrophages may cause the suppressed inflammatory response at Day 3. Although we investigated the suppressive inflammatory cytokine IL-10, we were unable to confirm the elevated production of this cytokine in the liver at Day 3 compared with Day 5 (Supplemental Fig. 1).

Although tissue macrophages and monocytes increased to reach a peak at Day 3 after injection, neutrophils increased rapidly and were reduced by Day 3. Interestingly, we found that neutrophil depletion exacerbated the αCD40-induced liver injury. In general, neutrophils have an effector function against several liver injury models, such as those involving carbon tetrachloride- and ischemic/perfusion-induced liver injury [26, 27]. These previous studies demonstrated that reactive oxygen from neutrophils is a key factor for hepatocyte damage. Our findings seem to be contradictory to the well-established paradigm that neutrophils induce tissue damage. However, the outcomes of αGr-1 treatment may vary depending on the liver injury models involved, as we have shown already that αGr-1 treatment partially protects against liver injury in hepatitis B virus transgenic mice [28, 29].

A recent report suggested that Gr-1^{high}CD11b^{+} cells suppress T cells in tumor-bearing mice [30] and that Gr-1^{high}CD11b^{low} polymononuclear cell–myeloid-derived suppressor cell populations have suppressive potential in the healthy spleen [31]. These reports suggest the possibility that liver injury is exacerbated by depletion of suppressive, Gr-1-positive cells. Furthermore, we need to confirm whether antibody-tagged neutrophils accumulate in the liver and whether Kupffer cells are activated by phagocytosis. In fact, we found that αGr-1 treatment induced the migration of macrophages and monocytes into the liver, and these cells produced large amounts of TNF-α, indicating that conclusive evidence for whether neutrophils have suppressive effects on this liver injury may require further investigations.

We further found that NKT cells participated in the αCD40-induced biphasic liver injury. NKT cells are particularly abundant in the liver, accounting for 20–30% of IHLs, and are thought to play roles in immunity against intracellular bacteria and parasites and certain tumors [8, 32]. It is well established that CD40 cross-linking induces DCs to up-regulate their expressions of CD40, B7.1, B7.2, and IL-12, which in turn, enhance NKT cell activation and cytokine production [32]. In this liver injury, NKT cells activated other inflammatory cells, including NK cells and macrophages, in the liver, as IFN-γ production by NK cells and TNF-α production by macrophages were apparently blocked in the liver of NKT KO mice. Consistent with the finding that macrophage recruitment was reduced in NKT KO mice, infiltration of the various macrophage subpopulations was also inhibited, indicating that NKT cells have an influence on macrophage differentiation following αCD40 injection. It is of note that NKT cells were secondarily activated by way of CD40 ligation on macrophages and DCs and that NKT KO mice appear to exhibit protection against inflammatory cell recruitment into the liver. These findings demonstrate the importance of NKT cells for the propagation of inflammatory liver disease.

In this study, we have demonstrated that IL-18 is involved in the late-phase liver injury. Although we found that IL-12 played a pivotal role in the early-phase liver injury, IL-18 was not necessary for liver injury to occur, as neutralization of IL-18 did not increase the serum ALT activity (Supplemental Fig. 5). IL-18 is known to induce NK and NKT cells to produce IFN-γ [12], but it

requires IL-12 to induce IFN-γ production by Th1 cells [11]. In keeping with these findings, we found that rIL-18 treatment rapidly induced intrahepatic NK cells to produce large amounts of IFN-γ and also to cause severe liver injury. Importantly, these effects did not involve TNF-α and did not require the recruitment of macrophages, monocytes, and neutrophils into the liver. More recently, intracellular microbial sensors have been identified, including NLRs [33, 34]. Some of the NLRs also sense nonmicrobial danger signals and form large cytoplasmic complexes called inflammasomes, which link the sensing of microbial products and metabolic stress to proteolytic activation of the proinflammatory cytokines IL-1β and IL-18. Therefore, in this model, the danger signals for early liver damage may trigger the activation of inflammasomes, resulting in the production of IL-18 and subsequent induction of liver damage.

In conclusion, the present results demonstrate that activation of intrahepatic macrophages can initiate a cascade of events that begins with the production of inflammatory cytokines and chemokines and leads to the activation of intrahepatic NK and NKT cells for the production of IFN-γ, all of which contribute to the recruitment of additional inflammatory cells to the liver (**Fig. 7**). We have shown that the interactions among macrophages, monocytes, neutrophils, and NKT cells participate efficiently and closely in the exacerbation of liver inflammation through cytokine and chemokine production. Further studies are required to identify the roles of the suppressive monocyte or neutrophil subpopulations in the liver injury, and clarification of the roles of these cell types will be useful in the treatment of various liver diseases.

AUTHORSHIP

K.K. planned the experimental project, and K.K., S.S., S.H., Y.H., T.H., and M.N. performed data analysis and wrote the paper. M.K. contributed data and comments about the manuscript.

ACKNOWLEDGMENTS

This study was supported by a grant-in-aid (B) from the Ministry of Education, Culture, Sports, Science and Technology of Japan (grant no. 20390203) and a grant-in-aid for specially promoted research on viral diseases from the Tokyo Metropolitan Government to K.K. We thank Dr. Francis V. Chisari (The Scripps Research Institute) for supporting this study and Dr. Antonius Rolink (Basel Institute for Immunology) for providing the anti-mouse agonistic CD40 mAb. We are also grateful to Drs. Toshinori Nakayama (Chiba University) and Masaru Taniguchi (RIKEN) for providing the Vα14 NKT KO mice.

REFERENCES

1. Akira, S., Uematsu, S., Takeuchi, O. (2006) Pathogen recognition and innate immunity. *Cell* **124,** 783–801.
2. Crispe, I. N. (2009) The liver as a lymphoid organ. *Annu. Rev. Immunol.* **27,** 147–163.
3. Crispe, I. N. (2003) Hepatic T cells and liver tolerance. *Nat. Rev. Immunol.* **3,** 51–62.
4. Banchereau, J., Briere, F., Caux, C., Davoust, J., Lebecque, S., Liu, Y. J., Pulendran, B., Palucka, K. (2000) Immunobiology of dendritic cells. *Annu. Rev. Immunol.* **18,** 767–811.
5. Munder, M., Mallo, M., Eichmann, K., Modolell, M. (1998) Murine macrophages secrete interferon γ upon combined stimulation with interleukin (IL)-12 and IL-18: a novel pathway of autocrine macrophage activation. *J. Exp. Med.* **187,** 2103–2108.
6. Zlotnik, A., Yoshie, O. (2000) Chemokines: a new classification system and their role in immunity. *Immunity* **12,** 121–127.
7. Wardle, E. N. (1987) Kupffer cells and their function. *Liver* **7,** 63–75.
8. Taniguchi, M., Harada, M., Kojo, S., Nakayama, T., Wakao, H. (2003) The regulatory role of Vα14 NKT cells in innate and acquired immune response. *Annu. Rev. Immunol.* **21,** 483–513.
9. Seino, K., Taniguchi, M. (2005) Functionally distinct NKT cell subsets and subtypes. *J. Exp. Med.* **202,** 1623–1626.
10. Van Kaer, L., Joyce, S. (2005) Innate immunity: NKT cells in the spotlight. *Curr. Biol.* **15,** R429–R431.
11. Nakanishi, K., Yoshimoto, T., Tsutsui, H., Okamura, H. (2001) Interleukin-18 regulates both Th1 and Th2 responses. *Annu. Rev. Immunol.* **19,** 423–474.
12. Okamura, H., Kashiwamura, S., Tsutsui, H., Yoshimoto, T., Nakanishi, K. (1998) Regulation of interferon-γ production by IL-12 and IL-18. *Curr. Opin. Immunol.* **10,** 259–264.
13. Kimura, K., Kakimi, K., Wieland, S., Guidotti, L. G., Chisari, F. V. (2002) Interleukin-18 inhibits hepatitis B virus replication in the livers of transgenic mice. *J. Virol.* **76,** 10702–10707.
14. Kimura, K., Kakimi, K., Wieland, S., Guidotti, L. G., Chisari, F. V. (2002) Activated intrahepatic antigen-presenting cells inhibit hepatitis B virus replication in the liver of transgenic mice. *J. Immunol.* **169,** 5188–5195.
15. Kimura, K., Moriwaki, H., Nagaki, M., Saio, M., Nakamoto, Y., Naito, M., Kuwata, K., Chisari, F. V. (2006) Pathogenic role of B cells in anti-CD40-induced necroinflammatory liver disease. *Am. J. Pathol.* **168,** 786–795.
16. Rolink, A., Melchers, F., Andersson, J. (1996) The SCID but not the RAG-2 gene product is required for S μ-S ε heavy chain class switching. *Immunity* **5,** 319–330.
17. Naito, M., Nagai, H., Kawano, S., Umezu, H., Zhu, H., Moriyama, H., Yamamoto, T., Takatsuka, H., Takei, Y. (1996) Liposome-encapsulated dichloromethylene diphosphonate induces macrophage apoptosis in vivo and in vitro. *J. Leukoc. Biol.* **60,** 337–344.
18. Gao, B., Jeong, W. I., Tian, Z. (2008) Liver: an organ with predominant innate immunity. *Hepatology* **47,** 729–736.
19. Guidotti, L. G., Chisari, F. V. (2001) Noncytolytic control of viral infections by the innate and adaptive immune response. *Annu. Rev. Immunol.* **19,** 65–91.
20. Jaeschke, H., Bajt, M. L. (2004) Critical role of CXC chemokines in endotoxemic liver injury in mice. *J. Leukoc. Biol.* **76,** 1089–1090, author reply 1091–1092.
21. Banchereau, J., Bazan, F., Blanchard, D., Briere, F., Galizzi, J. P., van Kooten, C., Liu, Y. J., Rousset, F., Saeland, S. (1994) The CD40 antigen and its ligand. *Annu. Rev. Immunol.* **12,** 881–922.
22. Cella, M., Scheidegger, D., Palmer-Lehmann, K., Lane, P., Lanzavecchia, A., Alber, G. (1996) Ligation of CD40 on dendritic cells triggers production of high levels of interleukin-12 and enhances T cell stimulatory capacity: T-T help via APC activation. *J. Exp. Med.* **184,** 747–752.
23. Grewal, I. S., Flavell, R. A. (1998) CD40 and CD154 in cell-mediated immunity. *Annu. Rev. Immunol.* **16,** 111–135.
24. Leenen, P. J., de Bruijn, M. F., Voerman, J. S., Campbell, P. A., van Ewijk, W. (1994) Markers of mouse macrophage development detected by monoclonal antibodies. *J. Immunol. Methods* **174,** 5–19.
25. Zhu, B., Bando, Y., Xiao, S., Yang, K., Anderson, A. C., Kuchroo, V. K., Khoury, S. J. (2007) CD11b+Ly-6C(hi) suppressive monocytes in experimental autoimmune encephalomyelitis. *J. Immunol.* **179,** 5228–5237.
26. Duffield, J. S., Forbes, S. J., Constandinou, C. M., Clay, S., Partolina, M., Vuthoori, S., Wu, S., Lang, R., Iredale, J. P. (2005) Selective depletion of macrophages reveals distinct, opposing roles during liver injury and repair. *J. Clin. Invest.* **115,** 56–65.
27. Luster, M. I., Simeonova, P. P., Gallucci, R. M., Bruccoleri, A., Blazka, M. E., Yucesoy, B. (2001) Role of inflammation in chemical-induced hepatotoxicity. *Toxicol. Lett.* **120,** 317–321.
28. Takai, S., Kimura, K., Nagaki, M., Satake, S., Kakimi, K., Moriwaki, H. (2005) Blockade of neutrophil elastase attenuates severe liver injury in hepatitis B transgenic mice. *J. Virol.* **79,** 15142–15150.
29. Sitia, G., Isogawa, M., Kakimi, K., Wieland, S. F., Chisari, F. V., Guidotti, L. G. (2002) Depletion of neutrophils blocks the recruitment of antigen-nonspecific cells into the liver without affecting the antiviral activity of hepatitis B virus-specific cytotoxic T lymphocytes. *Proc. Natl. Acad. Sci. USA* **99,** 13717–13722.
30. Dolcetti, L., Peranzoni, E., Ugel, S., Marigo, I., Fernandez Gomez, A., Mesa, C., Geilich, M., Winkels, G., Traggiai, E., Casati, A., Grassi, F., Bronte, V. (2010) Hierarchy of immunosuppressive strength among myeloid-derived suppressor cell subsets is determined by GM-CSF. *Eur. J. Immunol.* **40,** 22–35.
31. Greifenberg, V., Ribechini, E., Rossner, S., Lutz, M. B. (2009) Myeloid-derived suppressor cell activation by combined LPS and IFN-γ treatment impairs DC development. *Eur. J. Immunol.* **39,** 2865–2876.
32. Kronenberg, M. (2005) Toward an understanding of NKT cell biology: progress and paradoxes. *Annu. Rev. Immunol.* **23,** 877–900.
33. Martinon, F., Mayor, A., Tschopp, J. (2009) The inflammasomes: guardians of the body. *Annu. Rev. Immunol.* **27,** 229–265.
34. Pétrilli, V., Dostert, C., Muruve, D. A., Tschopp, J. (2007) The inflammasome: a danger sensing complex triggering innate immunity. *Curr. Opin. Immunol.* **19,** 615–622.

KEY WORDS:
neutrophil · macrophage · NKT cell · chemokine · IL-18

Biochemical and Biophysical Research Communications 391 (2010) 1421–1426

Contents lists available at ScienceDirect

Biochemical and Biophysical Research Communications

journal homepage: www.elsevier.com/locate/ybbrc

IL-6 and IFN-α from dsRNA-stimulated dendritic cells control expansion of regulatory T cells

Nobuhiko Kubota [b,a,1], Takashi Ebihara [a,1,2], Misako Matsumoto [a], Satoshi Gando [b], Tsukasa Seya [a,*]

[a] Department of Microbiology and Immunology, Hokkaido University Graduate School of Medicine, Sapporo 060-8638, Japan
[b] Department of Anesthesiology and Critical Care Medicine, Hokkaido University Graduate School of Medicine, Sapporo 060-8638, Japan

ARTICLE INFO

Article history:
Received 8 December 2009
Available online 22 December 2009

Keywords:
TICAM-1 (TRIF)
Interferon-alpha
IL-6
Dendritic cells
Regulatory T cells (Treg)

ABSTRACT

Foxp3$^+$CD4$^+$ regulatory T cells (Treg) control not only autoimmunity but also the effective immune response against RNA virus infections, which produces virus-derived double-stranded RNA (dsRNA). To induce effective anti-viral immunity, it is a key issue to learn how Treg respond to dsRNA *in vitro* and *in vivo*. We here showed that synthetic dsRNA, polyI:C, caused peripheral expansion of functional Treg in a TICAM-1- and IL-6-dependent manner *in vivo*. PolyI:C did not expand Treg directly, but promoted the expansion of naturally occurring Treg indirectly through IL-6 produced from dendritic cells (DCs). In addition, the expansion of Treg by IL-6 was inhibited by IFN-α from polyI:C-stimulated DCs. These data suggest that the balance of IL-6 and IFN-α in the region of RNA virus infection may determine the number of peripheral Treg, which affects the effective immune responses against viruses.

Introduction

CD4$^+$CD25$^+$ regulatory T cells (Treg) are crucial to control autoimmunity and maintain immunological self-tolerance [1,2]. The development and function of Treg is controlled by the forkhead/winged helix transcription factor Foxp3 [1,2]. Naturally occurring Treg cells (nTreg) are arising from thymus, while induced Treg (iTreg) are converted from peripheral CD4$^+$CD25$^-$ T cells [3,4]. Both Treg constitute 5–15% of peripheral CD4$^+$ cells and control not only immunological self-tolerance but also immune response to pathogens [4,5]. In RNA virus infections, during which virus-specific RNA patterns are generated in infected cells, many researchers suggest that peripheral Treg are increased to cause persistent infection of viruses [6].

Innate and adaptive immune responses against RNA virus infections are controlled by dendritic cells (DCs) [7]. For sensing virus-derived RNAs, murine DCs are armed with Toll-like receptor (TLR)3, TLR7 and TLR8, and RIG-I-like receptors (RLRs), which include RIG-I, MDA5 and LGP2 [8,9]. Myeloid DCs express TLR3 and TLR8, whereas plasmacytoid DCs (pDCs) exclusively express TLR7 [10]. TLR7 and TLR8 recognize single-stranded RNAs (ssRNAs), whereas TLR3 detects virus-derived dsRNAs. These three TLRs reside in the endosome to encounter exogenous RNAs [11]. While TLR7 and TLR8 require MyD88 as an adaptor molecule for its signaling, TLR3 recruits TIR-containing adaptor molecule (TICAM)-1 (also called TRIF) which induces type I IFN through IRF-3 activation and inflammatory cytokines (IL-6, TNF-α, etc.) by NF-κB activation [11].

In contrast, RLRs are distributed in a variety of cells including DCs. RIG-I and MDA5 are cytosolic sensors of RNAs and interact with a downstream mitochondrial protein, IFN-β promoter stimulator 1 (IPS-1, also called MAVS/VISA/CARDIF), which activates IRF-3 (interferon-regulatory factor 3), NF-κB (nuclear factor-kappaB), and AP-1 (activator protein 1) and induces IFN-β and inflammatory cytokines [9].

TLRs are also known to be expressed on CD4$^+$CD25$^+$Foxp3$^+$ Treg and directly modulate the proliferation and suppressive functions [12,13]. CD4$^+$CD25$^+$ Treg selectively expresses TLR4, TLR5, TLR7 and TLR8 [12]. In contrast, TLR1, TLR2, TLR3 and TLR6 are more widely expressed on CD4$^+$ T cells. TLR8 ligand is known to work on Treg directly and reverse the Treg suppressive activity [14]. However, the response of Treg against dsRNA is poorly understood neither *in vivo* nor *in vitro*.

Here, we examined the effect of synthetic dsRNA, polyI:C, on Treg expansion. PolyI:C increased peripheral Treg in a bone marrow-derived DC (BMDC)-dependent manner *in vivo* and *in vitro*.

Abbreviations: Treg, regulatory T cells; DC, dendritic cell; BMDC, bone marrow-derived dendritic cell; TICAM-1, Toll-interleukin 1 receptor domain (TIR)-containing adaptor molecule; Foxp3, forkhead box P3; RIG-I, retinoic acid-inducible gene I; MDA5, melanoma differentiation-associated gene 5; IPS-1, IFN-β promoter stimulator 1; RLRs, RIG-I-like receptors.

* Corresponding author. Address: Department of Microbiology and Immunology, Hokkaido University Graduate School of Medicine, Kita-15, Nishi-7, Kita-ku, Sapporo 060-8638, Japan. Fax: +81 11 706 7866.
E-mail address: seya-tu@pop.med.hokudai.ac.jp (T. Seya).
[1] These authors equally contributed to this work.
[2] Present address: Howard Hughes Medical Institute, Washington University School of Medicine, St. Louis, MO 63110, USA.

0006-291X/$ - see front matter © 2009 Elsevier Inc. All rights reserved.
doi:10.1016/j.bbrc.2009.12.081

The polyI:C plus BMDCs expanded Treg in a TICAM-1- and IL-6-dependent manner. We also found that IFN-α from BMDCs suppressed the proliferation of nTreg. These indicate that myeloid DCs play a regulatory role in nTreg proliferation by producing IL-6 and IFN-α upon polyI:C stimulation.

Materials and methods

Mice and reagents. C57BL/6J mice and IL-6$^{-/-}$ mice were purchased from Charles River (Yokohama, Japan). TICAM-1$^{-/-}$ mice were generated in our laboratory [15]. IFNAR$^{-/-}$ mice were kindly provided by Dr. T. Taniguchi (University of Tokyo, Tokyo, Japan). All mice were bred and housed pathogen-free in our facility with the approval of the Hokkaido University Animal Experiments Committee. PolyI:C was purchased from GE Healthcare (Chalfont St. Giles, UK). Recombinant murine IL-2 was purchased from Pepro Tech (Rocky Hill, NJ, USA). Recombinant murine IL-6 (097-04431) and IFN-α (130-093-131) were from Wako Pure Chemical Industries, Ltd. (Osaka, Japan) and Miltenyi Biotec (Bergisch Gladbach, Germany), respectively. FITC anti-Foxp3 mAb (11-5773), PE anti-CD4 mAb (12-0042), PE-Cy5 anti-CD4 mAb (15-0042), FITC Rat IgG2a isotype control (11-4321), PE Rat IgG2a isotype control (12-4321), PE-Cy5 Rat IgG2a isotype control (15-4031) and functional grade anti-CD3 mAb (14-0033) were from eBioscience (San Diego, CA, USA).

Cells. CD4$^+$CD25$^+$ (Treg) cells and CD4$^+$CD25$^-$ cells were purified from mouse splenocytes using a MACS CD4$^+$CD25$^+$ Regulatory T Cell Isolation Kit (Miltenyi Biotec). BMDCs were generated from bone marrow cells by culture for 6 days in RPMI 1640 medium supplemented with 10% heat-inactivated FCS (JRH Biosciences, Lenexa, KS, USA) in the presence of 500 IU/ml recombinant murine granulocyte macrophage colony-stimulating factor (Pepro Tech). Sometimes, BMDCs (1×10^6/ml) were incubated with or without 50 μg/ml polyI:C for 24 h and the supernatants were collected for ELISA. The concentrations of cytokines (IL-6 and IFN-α) were measured by commercial ELISA kits (Invitrogen, Carlsbad, CA, USA; PBL Biomedical Laboratories, Piscataway, NJ, USA). PolyI:C (1.25 mg/ml:200 μl) was injected intraperitoneally and inguinal lymph nodes were excised for FACS analysis. The ratio of Treg cells (CD4$^+$Foxp3$^+$/CD4$^+$) was determined by analysis from FlowJo (Tree Star Inc., OR, USA).

In vivo polyI:C administration. PolyI:C (250 mg/200 ml) or control phosphate-buffered saline (PBS) was intraperitoneally administered into mice twice at three days interval. Twenty-four hours after the last injection, the spleen and lymph nodes were extracted and total cell numbers were counted. Then, the numbers of the CD4$^+$ and CD4$^+$Foxp3 populations were assessed by FACS as described [16] and the scales of the CD4$^+$ and CD4$^+$Foxp3 fractions were evaluated.

Treg proliferation assay. Treg cells (5×10^4) were cultured in 96 wells round bottom-shaped plate in the presence of 1 μg/ml anti-CD3 antibody and 100 U/ml recombinant IL-2 with or without 50 μg/ml polyI:C for 2 days. For the Treg/BMDCs coculture, 1×10^6 BMDCs were added to the well. Occasionally, IL-6 (10 ng/ml) and/or IFN-α (10–10^4 IU/ml) were added to the culture. During the last 6 h of culturing, [^{3}H]thymidine (1 μCi/well) was mixed in the culture medium. The cells and medium were harvested separately by cell-harvester, and the radioactivity was measured by a liquid scintillation counter (Aloca, Tokyo, Japan).

Treg suppression assay. Treg cells were incubated with BMDCs for 2 days as described above, and subsequently only the Treg cells were resorted by MACS system. Splenocytes (1×10^5) were treated with mytomycin C (20 μg/ml, 45 min) and cultured with freshly isolated CD4$^+$CD25$^-$ T cells (responder, 2.5×10^4) for 2 days. The ratio of CD4$^+$CD25$^-$/CD4$^+$CD25$^+$ was indicated in the figure. The proliferation of responder cells was measured by [^{3}H]thymidine uptake assay.

Results

PolyI:C induces the proliferation of Treg in vivo and in vitro

To examine the effect of dsRNA on Treg function *in vivo*, we administered polyI:C intraperitoneally into mice and evaluated the absolute numbers and increase of Treg cells (CD4$^+$Foxp3$^+$) compared to CD4$^+$ T cells in the inguinal lymph nodes (LN) and spleen. Treg numbers were increased after polyI:C administration in LN (Fig. 1A and B), and spleen (data not shown). The results were confirmed with additional experiments (Fig. S1) where the numbers of the Treg cells in spleens and indicated lymph nodes were counted with mice treated with or without polyI:C as in Fig. 1A.

To investigate the mechanisms of Treg expansion by polyI:C, we first examined whether polyI:C acts on nTreg cells (CD4$^+$CD25$^+$ T cell) directly as a proliferation stimulator or whether polyI:C converts CD4$^+$CD25$^-$ T cells into CD4$^+$CD25$^+$ T cells (iTreg) *in vitro*. We observed that polyI:C stimulated Treg to activate the transcription factors downstream the TLR3/TICAM-1 pathway (data not shown), although polyI:C neither elicited proliferation of nTreg cells (Fig. 1C) nor induced CD4$^+$CD25$^+$ T cells from CD4$^+$CD25$^-$ T cells *in vitro* (Fig. S2). These results suggest that polyI:C may act on cells other than Treg to initiate Treg expansion.

To see if polyI:C expands Treg through myeloid DCs, we cultured nTreg and BMDCs in the presence of polyI:C *in vitro*. BMDC is the most likely candidate because it has been reported that LPS-matured BMDCs expand nTreg [16–18], and polyI:C induces maturation of BMDCs through TLR3 [7,19]. As a result, polyI:C plus BMDCs triggered Treg expansion (Fig. 1D). We next injected polyI:C-stimulated BMDCs intraperitoneally and examined the ratio of Treg/CD4$^+$ cells in LN. PolyI:C-stimulated BMDCs actually mediated peripheral Treg expansion *in vivo* (Fig. 1E). These results suggest that polyI:C-stimulated BMDCs help Treg expand *in vivo* and *in vitro*.

The Treg proliferation by polyI:C-stimulated DCs requires TICAM-1 signal and IL-6

Next we examined whether IL-6 induced by the TLR3/TICAM-1 pathway influences the Treg maintenance using IL-6$^{-/-}$ and TICAM-1$^{-/-}$ mice. When we injected polyI:C into IL-6$^{-/-}$ mice or TICAM-1$^{-/-}$ mice, there was no significant increase of Treg in LN (Fig. 2A). Consistent with our previous report [15], we found that TICAM-1$^{-/-}$ mice impaired full production of IL-6 in response to polyI:C *in vitro* and *in vivo* (Fig. 2B). These results suggest that the Treg expansion by polyI:C injection may require IL-6, which is produced through TICAM-1 signaling.

To see if IL-6- or TICAM-1-signaling is essential for polyI:C-stimulated BMDCs to expand Treg, Treg cells were cultured with BMDCs from TICAM-1$^{-/-}$, IL-6$^{-/-}$ or wild-type mice with or without polyI:C. The Treg expansion by polyI:C was largely suppressed with TICAM-1$^{-/-}$ BMDCs and more severely abrogated in IL-6$^{-/-}$ BMDCs (Fig. 2C). When we checked the IL-6 production from each culture, the Treg proliferation appeared to be associated with the IL-6 production from BMDCs (Fig. 2D). To see if the reconstitution of IL-6 can recover the reduced Treg proliferation by TICAM-1$^{-/-}$ or IL-6$^{-/-}$ BMDCs plus polyI:C, IL-6 was added into the BMDC/Treg coculture. The exogenous IL-6 could recover the Treg proliferation by BMDCs from TICAM-1$^{-/-}$ and IL-6$^{-/-}$ mice in the presence of polyI:C (Fig. 2E).

These data suggest that the Treg proliferation by BMDC plus polyI:C is dependent on IL-6 produced by BMDCs through the TLR3/TICAM-1 pathway.

DC produced IFN-α to inhibit the Treg expansion induced by IL-6

Next we cultured Treg with BMDCs with or without polyI:C in the presence or absence of exogenous IL-6. Treg was expanded

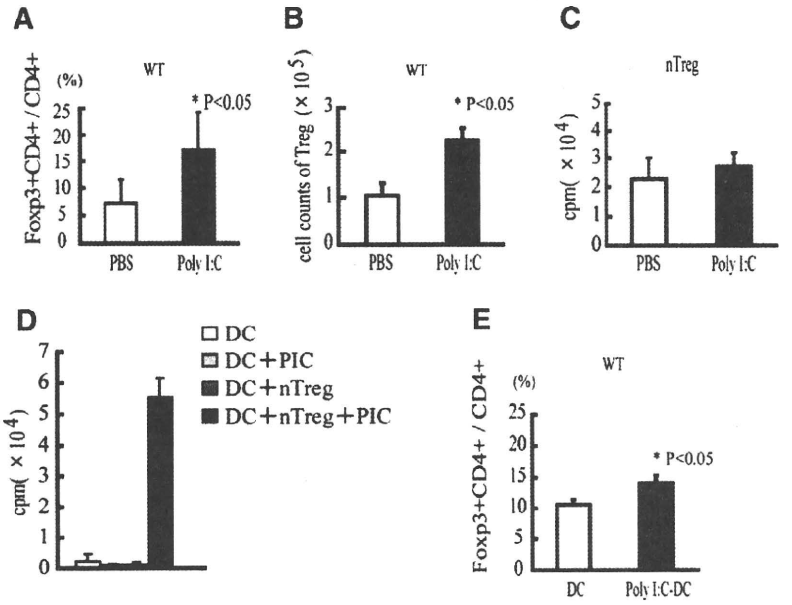

Fig. 1. PolyI:C induces the proliferation of Treg *in vivo* and *in vitro*. (A,B) C57BL/6J wild-type (WT) mice were intraperitoneally injected with polyI:C (1.25 mg/ml:200 μl) or PBS twice every 3 days throughout the experiments. Inguinal lymph nodes were excised, and the ratio of $CD4^+Foxp3^+$ /$CD4^+$ T cells (A) and the absolute number of $CD4^+Foxp3^+$ (B) cells were determined by FACS at 1 day after the final administration. (C) Freshly isolated $CD4^+CD25^+$ Treg (5×10^4) from WT mice were cultured in the presence of 1 μg/ml anti-CD3 antibody and 100 U/ml recombinant IL-2 with or without 50 μg/ml polyI:C. The proliferation was determined by $[^3H]$thymidine uptake after 2 day culture. There was no statistical difference between them. (D) As in (C), but 1×10^6 WT BMDCs were added to each well. (E) The ratio of $CD4^+Foxp3^+/CD4^+$ T cells in LN was analyzed at 24 h after injection of non-treated BMDCs (DC) or BMDCs incubated with 50 μg/ml polyI:C (polyI:C DC) for 24 h. Data represented the mean ± SD of three independent experiments.

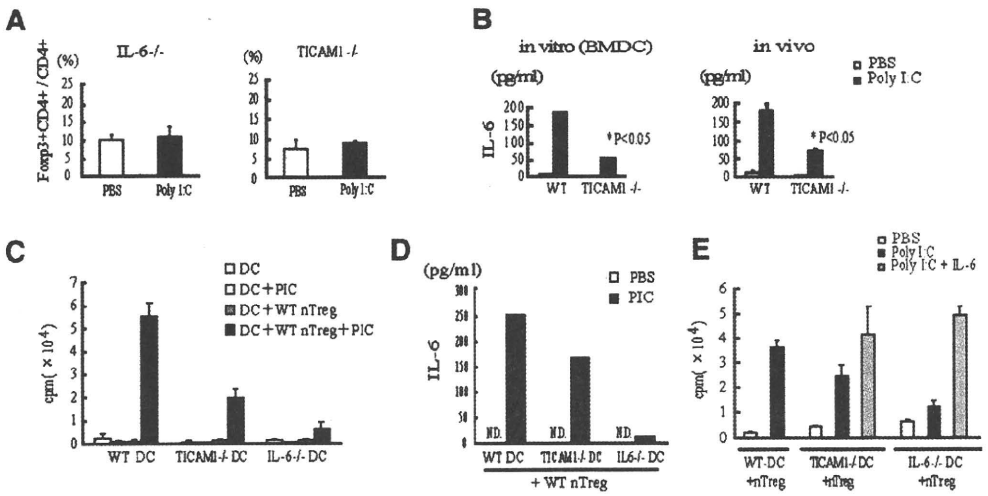

Fig. 2. The Treg proliferation by polyI:C plus BMDCs requires TICAM-1 signaling and IL-6. (A) TICAM-$1^{-/-}$ mice and IL-$6^{-/-}$ mice were intraperitoneally injected with polyI:C or PBS as in Fig. 1A and the ratio of $Foxp3^+CD4^+$ Treg/$CD4^+$ T cells was determined. There was no statistical difference between PBS-group and polyI:C-group. (B) The supernatants and sera were assayed for the production of IL-6. BMDCs were incubated with or without 50 μg/ml polyI:C for 24 h, and the supernatants were collected. The sera were collected at 24 h after injection of polyI:C. (C) BMDCs from WT, TICAM-$1^{-/-}$ or IL-$6^{-/-}$ mice (1×10^6) were cultured in the presence of 1 μg/ml anti-CD3 antibody and 100 U/ml recombinant IL-2 with or without Treg (5×10^4) from WT mice in the presence or absence of 50 μg/ml polyI:C. The proliferation was determined by $[^3H]$thymidine uptake after 2 day culture. (D) As in (C), but Treg from WT mice were cultured with BMDCs from WT, TICAM-$1^{-/-}$ or IL-$6^{-/-}$ mice. After 24 h culture, supernatants were collected and measured for IL-6 production. (E) As in (C), but Treg from WT mice were cultured with BMDCs from WT, TICAM-$1^{-/-}$ or IL-$6^{-/-}$ mice with or without 50 μg/ml polyI:C or polyI:C plus 10 ng/ml IL-6. The proliferation was determined by $[^3H]$thymidine uptake after 2 day culture. Data represented the mean ± SD of three independent experiments.

by polyI:C plus BMDCs as described above, and Treg proliferated better in the presence of both polyI:C and IL-6 (Fig. 3A). However, interestingly, we found that Treg was expanded much better by IL-6 alone (Fig. 3A). This indicates that Treg-proliferation induced by IL-6 seems to be suppressed by polyI:C.

Since type I IFN is a critical factor for Th1-dominant CD4 response against dsRNA [20], we hypothesized that IFN-α produced by polyI:C-stimulated BMDCs may induce proliferation of Th1 cells and suppress the Treg-proliferation induced by IL-6 from polyI:C-stimulated BMDCs. To test this possibility, we first measured

IFN-α production in serum from polyI:C-injected wild-type and TICAM-1$^{-/-}$ mice. As shown in Fig. 3B left, IFN-α production was intact in TICAM-1$^{-/-}$ mice after the polyI:C injection. IFN-α production in culture supernatants was also similar between BMDCs from wild-type mice stimulated with polyI:C and those from TICAM-1$^{-/-}$ mice (Fig. 3B right). The results infer that cytoplasmic MDA5 rather than TLR3 preferentially induces IFN-α in response to polyI:C in our setting *in vivo* and *in vitro*.

Next, we checked if exogenous IFN-α could inhibit the Treg proliferation. When Treg were cultured with BMDCs in the presence of polyI:C and graded doses of IFN-α, IFN-α actually inhibited the Treg proliferation in a dose-dependent manner (Fig. 3C). IFN-α also abolished the proliferation of Treg induced by BMDCs plus IL-6 in a dose-dependent manner (Fig. 3D). To see if IFN-α derived from BMDCs is responsible for the suppression of the Treg-proliferation induced by IL-6 from polyI:C-stimulated BMDCs, we used IFNAR$^{-/-}$ BMDCs which barely amplify type I IFN production but can activate the MDA5/IPS-1 pathway [15]. We found that IFNAR$^{-/-}$ BMDCs did not suppress IL-6-mediated Treg expansion induced by polyI:C-stimulated BMDCs (Fig. 3E). These indicate that IFN-α has negative effect on Treg-proliferation induced by IL-6 derived from polyI:C-stimulated BMDCs.

We next examined which cells were required to be stimulated by these two cytokines for Treg expansion. BMDCs were treated with mitomycin C after stimulation with IL-6 and/or IFN-α and co-cultured with Treg cells in the presence of IL-6 and/or IFN-α. In this series of experiments, we could not observe any effects of IL-6 and IFN-α on direct Treg expansion (Fig. 3F), suggesting that IL-6 and IFN-α modulate the BMDC function to adjust the Treg number in the periphery.

Treg cells expanded by polyI:C-stimulated DCs are functional in vitro

Finally, we tested whether polyI:C-stimulated BMDC-driven Treg cells sustain the suppressive activity against responder cells. Treg suppressive activity was not altered after co-culturing with BMDC in the presence of polyI:C, IL-6 and IFN-α (Fig. 4A and B). Hence, IL-6 and type I IFN from BMDCs control the number of Treg cells but not the ability to suppress naïve T cells.

Discussion

We demonstrated in this study that BMDCs control proliferation of Treg by secreting IL-6 and IFN-α after sensing dsRNA. Although IFN-α negatively acts on Treg expansion, IL-6 overwhelmed the inhibitory effects of IFN-α on Treg. As a result, dsRNA caused proliferation of Treg with competent suppressive activity. Although the cytoplasmic polyI:C response governs the level of type I IFN in BMDCs and *in vivo*, the TICAM-1 pathway in BMDCs participates in proliferation of Treg in the periphery.

IFN-α is a main anti-viral cytokine that induces many IFN-inducible gene products, such as OAS, Mx1, and ISG15, leading to the limitation of RNA virus replication [8,20]. Here we describe a new anti-viral function of IFN-α. IFN-α suppressed Treg-proliferation induced by IL-6 derived from polyI:C-treated myeloid DCs. Treg cells suppress DC function and T-cell activation as well as NK activation [4]. Therefore, type I IFN including IFN-α may work to enforce the anti-viral cellular immunity by inhibiting Treg proliferation. In RNA virus infections, not only myeloid DCs but also pDCs and other virus-infected cells systematically produce type I IFN [8], which can contribute to the inhibition of Treg proliferation *in vivo*. Our data suggest that the tissue-specific cytokine balance between IL-6 and IFN-α is a determinant factor of Treg expansion.

IFN-α and IL-6 are known to up-regulate co-stimulatory molecules such as CD80 and CD86 on DCs. We have shown that CD8$^+$CD205$^+$ splenic DCs in the steady state induce antigen-specific Foxp3$^+$ Treg from Foxp3$^-$CD25$^-$CD4$^+$ T cells using endogenous TGF-β [21]. Thus, specific resident DC subsets govern iTreg induction. Our present data speculate that bone marrow-supplied DC subsets in the inflammatory states also regulate the peripheral Treg balance. The Treg control by polyI:C-stimulated BMDCs is IL-6- and IFN-α-dependent and may modally distinct from that of the splenic DCs. Although what pathogenic states preferentially enhance nTreg expansion remain to be elucidated, it is interesting

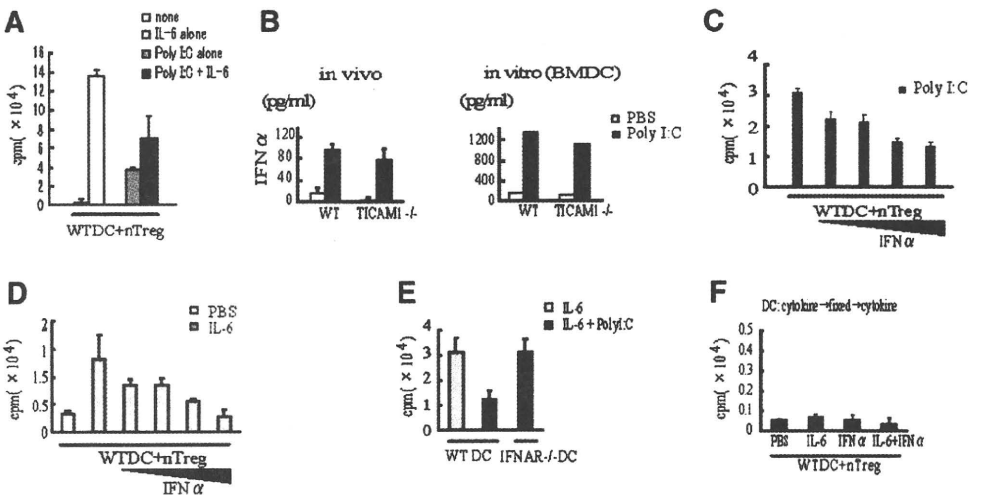

Fig. 3. Effect of IFN-α and IL-6 on Treg expansion. (A) As in Fig. 2C, but Treg from WT mice were cultured with WT BMDCs with or without 50 μg/ml polyI:C or 10 ng/ml IL-6. The proliferation was determined by [^{3}H]thymidine uptake after 2 day culture. (B) As in Fig. 2B, but the supernatants and sera were assayed for production of IFN-α. (C) As in (A), but graded doses of IFN-α (10–10^4 IU/ml) was added to the culture with 50 μg/ml polyI:C. The proliferation was determined by [^{3}H]thymidine uptake after 2 day culture. (D) As in (C), but graded doses of IFN-α (10–10^4 IU/ml) was added to the culture with or without IL-6 (10 ng/ml). The proliferation was determined by [^{3}H]thymidine uptake after 2 day culture. (E) As in Fig. 2C, but Treg from WT mice were cultured with BMDCs were from IFNAR$^{-/-}$ or WT mice in the presence of 10 ng/ml IL-6 with or without 50 μg/ml polyI:C. The proliferation was determined by [^{3}H]thymidine uptake after 2 day culture. (F) WT BMDCs were incubated with IFN-α (10^3 IU/ml) and/or IL-6 (10 ng/ml) for 24 h and fixed by mitomycin C subsequently. Then, nTreg were cultured with these fixed BMDCs for 2 days in the presence of the same cytokines used with stimulating BMDCs. Data represented the mean ± SD of three independent experiments.

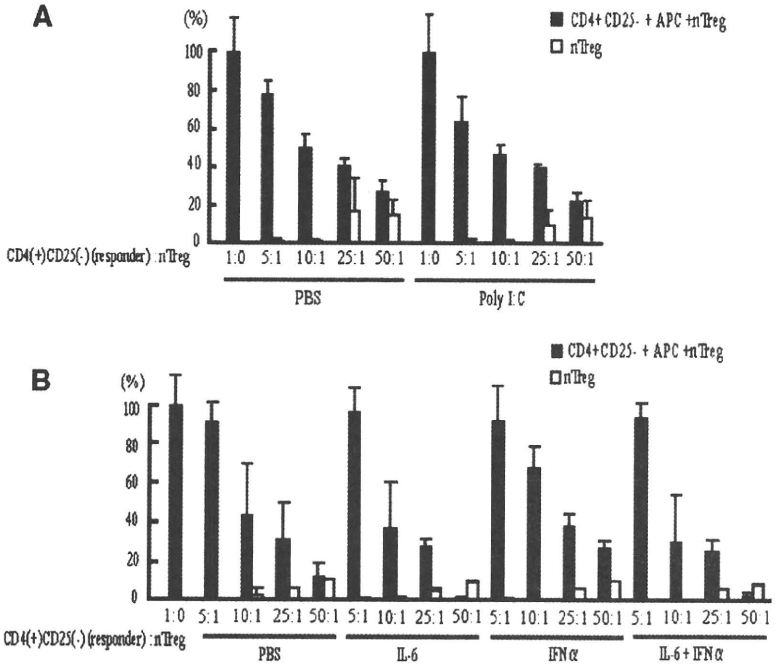

Fig. 4. Treg expanded by polyI:C plus BMDCs are suppressive *in vitro*. (A) Treg were isolated after 2-day culture with BMDCs in the absence (PBS) or presence of 50 μg/ml polyI:C (polyI:C). Then, these nTreg (suppressor) were cultured with freshly isolated $CD4^+CD25^-$ T cells (responder, 2.5×10^4), mitomycin C-treated splenocytes (1×10^5) and anti-CD3 Ab for 2 days. The proliferation was determined by [^{3}H]thymidine uptake after 2 day culture. (B) As in (A), but Treg were cultured with BMDCs with or without IL-6 (10 ng/ml) or IFN-α (10^3 IU/ml), and used for the suppression assay.

that IL-6 and IFN-α differentially regulate myeloid DC function to stimulate nTreg.

Our data showed that peripheral expansion of Treg is dependent on IL-6 induced by polyI:C, though an *in vivo* Treg increase is less efficient than *in vitro*. IL-6 has been shown to play a multifarious role to expand and maintain Treg. IL-6 has contrasting effects against nTreg and iTreg [15,17,22,23]. IL-1 and IL-6 production by myeloid DC is required to enhance nTreg proliferation after LPS stimulation [17]. Treg can be induced from $CD4^+CD25^-$ T cells, and peripheral Treg number is controlled in the balance between iTreg and pro-inflammatory IL-17-secreting cells (Th17) [5]. IL-6 and TGF-β together induce the differentiation of Th17 cells from naive T cells [24,25]. Moreover, IL-6 can convert nTreg to Th17 cells [26]. Therefore, in this line, pro-inflammatory effects of IL-6 promote differentiation of Th17, but not that of Treg.

In our experiments, $CD4^+CD25^+Foxp3^+$ cells were not induced from $CD4^+CD25^-$ T cells by function of polyI:C-stimulated BMDCs (Fig. S2). However, in contrast, the polyI:C-stimulated BMDCs could expand Treg (Fig. 1D). Moreover, although TGF-β is a key cytokine for differentiation of iTreg and Th17, serum level of TGF-β did not increase after i.p. polyI:C administration, and BMDC did not produce TGF-β (data not shown). Therefore, we prefer the interpretation that the peripheral increase of Treg numbers by polyI:C is due to the proliferation of nTreg *in vivo*. However, since there is no marker to distinguish nTreg from iTreg, we have no way to examine the actual proportion of these two subsets *in vivo*.

TLR ligands including TLR2, TLR4, TLR5, and TLR8 directly modulate the Treg suppressive function and number of nTreg [12–14]. TLR-signaling through TLR2 or TLR4 in nTreg enhances proliferation and suppressive activity of nTreg [12,13]. In our investigation, nTreg did not proliferate in direct response to polyI:C, a TLR3 ligand alone; however, polyI:C enhances nTreg expansion in the presence of BMDCs by the DC TICAM-1-mediated pathway. Previous reports showed that TLRs in BMDCs control Treg expansion and function, using a TLR4 ligand, LPS [16–18]. Since TLR4 signaling induces type I IFN and IL-6 mainly through the TICAM-1 pathway, it is possible that these two cytokines produced by TLR4 signaling may also exert its suppressive or enhancing effects on Treg proliferation as in the case of polyI:C stimulation.

It is an intriguing idea to control Treg for the induction of effective anti-viral immunity against persistent RNA virus infections. We found that IFN-α-treated mDCs actually suppress Treg growth, whereas signaling of IL-6 on mDCs overcomes the IFN-α-mediated suppression of Treg expansion. Investigating how Treg are controlled by these two cytokines may shed light on developing a new way to induce powerful anti-virus immunity on RNA virus infection.

Acknowledgments

We are grateful to Dr. Sayuri Yamazaki (Hokkaido Univ., Sapporo) for her invaluable discussions. This work was supported in part by the Ministry of Education, Science, and Culture and the Ministry of Health, Labor, and Welfare of Japan

Appendix A. Supplementary data

Supplementary data associated with this article can be found, in the online version, at doi:10.1016/j.bbrc.2009.12.081.

References

[1] J.M. Kim, J.P. Rasmussen, A.Y. Rudensky, Regulatory T cells prevent catastrophic autoimmunity throughout the lifespan of mice, Nat. Immunol. 8 (2007) 191–197.
[2] S. Sakaguchi, T. Yamaguchi, T. Nomura, M. Ono, Regulatory T cells and immune tolerance, Cell 133 (2008) 775–787.
[3] W. Chen, W. Jin, N. Hardegen, K.J. Lei, L. Li, N. Marinos, G. McGrady, S.M. Wahl, Conversion of peripheral $CD4^+CD25^-$ naive T cells to $CD4^+CD25^+$ regulatory T cells by TGF-beta induction of transcription factor Foxp3, J. Exp. Med. 198 (2003) 1875–1886.